

# Impact of medical radionuclide discharges on people and the environment

J. Vives i Batlle<sup>1</sup> (✉), L. Sweeck<sup>1</sup>, F. Fiengo Pérez<sup>2</sup>

<sup>1</sup>Belgian Nuclear Research Centre (SCK•CEN), Boeretang 200, 2400 Mol, Belgium. Tel: +32 (0)14 33 88 05, Fax: +32 (0)14 32 10 56, e-mail: jordi.vives.i.batlle@sckcen.be

<sup>2</sup>Aquafin NV, Dijkstraat 8, 2630, Aartselaar, Belgium

Note: This is a preprint version of the article as originally submitted in the Journal of Environmental Radioactivity (DOI: <https://doi.org/10.1016/j.jenvrad.2023.107362>)

## ABSTRACT

We present a novel methodology to dynamic calculate dose rates to non-human biota from hospital-released radionuclides reaching the environment through waste water treatment plants (WWTPs), using the biokinetic model D-DAT for aquatic biota, applied to <sup>18</sup>F, <sup>123</sup>I, <sup>131</sup>I, <sup>153</sup>Sm, <sup>99m</sup>Tc and <sup>201</sup>Tl. We have also developed a method to calculate doses to WWTP workers and farmers from agricultural practices. This proof-of-concept study uses a calculated generic source term of radionuclide levels in the Belgian Molve Nete River during the year 2018. The dose rates to non-human biota calculated for this scenario, which are calculated under conservative assumptions, are well below ERICA predicted no effects dose rate to wildlife of 10  $\mu\text{Gy h}^{-1}$ . For humans, the exposures are also very low, approaching a trivial value of the dose rate of 10  $\mu\text{Sv y}^{-1}$  in most cases. This work identifies important data gaps and areas of uncertainty in the assessment of radiopharmaceutical effluents. The study, which is part of the EC project SINFONIA, paves the way for a possible pan-European screening assessment methodology with the possibility to perform consistently assessments of the impact of radiopharmaceuticals on people and the environment. This is particularly relevant since discharges of radiopharmaceuticals in rivers are on the increase and it is necessary to explicitly demonstrate that people and the environment are adequately protected.

Keywords: Hospitals; Radiological impact assessment; Molve Nete; Radiopharmaceuticals; Wildlife; Water treatment plant.

## 1. INTRODUCTION

Radiopharmaceuticals are broadly used for diagnostic purposes, for treatment of cancer and other diseases. After their use in hospitals, radioactive effluents are collected in special tanks until acceptable activity levels are reached for their release into the sewer system. Then, they are conveyed through the sewer system to wastewater treatment plants (WWTPs) for further standard 24 - 48 h treatment, whereupon they are released into rivers. There they come in contact with aquatic life and people via ingestion and the external exposure pathways.

With the general increase of radiopharmaceutical use, including the approval of new treatments, releases to WWTPs and watercourses are on the increase. The radionuclides involved typically include short-lived  $\gamma$ -ray emitters used for imaging and diagnostics, such as  $^{99}\text{Tc}$  (IAEA, 2009), but also longer-lived  $\beta$ -emitting radionuclides that are used in therapeutic treatments, such as  $^{131}\text{I}$  (Veliscek Carolan et al., 2011), to which one must add a variety of novel isotopes (including  $\alpha$ -emitters) arising from recently approved radiopharmaceuticals and novel techniques in nuclear medicine, which have experienced a remarkable increase in recent times (Vives i Batlle et al., 2022).

Radiological impact assessments for these environmental releases are seldom conducted and environmental parameter data for specific radionuclides are lacking. Some unusual sewer-WWTP-aquatic dispersion pathways are involved, and this leads to both over-conservatism and uncertainty in assessments. Assessment uncertainties are contributed to by the fact that environmental monitoring is not often performed, and there is a lack of environmental parameter values to represent the relevant uptake, bioaccumulation and dispersion pathways. Radiation doses to WWTP workers, the public and the environment are presumed to be low due to the short half-life of most of the radionuclides (Martínez et al., 2018), but this is not a given for all situations/radionuclides and there is a need to explicitly prove protection of people and the environment for a wider variety of radionuclides and assessment cases, including routine and accidental releases.

From the environmental perspective, the highest priority is to produce special models for dose assessment of radionuclide releases from hospitals to the environment via WWTPs, not only for impact on members of the public but also for wildlife. The reason to include wildlife is that the International Commission on Radiation Protection (ICRP) has established that, in addition to humans, the environment should similarly be protected from deleterious effects of radiation (ICRP, 2008, 2014, 2017). The goal to protect the environment is motivated by a significant evolution of thought based on both moral and scientific grounds, debunking the old statement that “if humans are protected, the environment is also protected”.

In Belgium, there is a lack of radiological impact assessment of current as well as future medical releases, and hospitals are not always forthcoming with information on their waste disposal practices. This is because licensing usually does not require hospitals to sample or do monitoring of the

environment and there is no notification procedure for outside releases. To address this, between 2012 and 2014, automatic measuring stations were installed by the Federal Agency for Nuclear Control in some of the treatment plants that receive wastewater containing radiopharmaceuticals (FANC, 2015). The measurements show that, in the influents at the inlet of the WWTPs,  $^{99m}\text{Tc}$  and  $^{131}\text{I}$  (which typically appear as discontinuous discharges, or “spikes”) are often detected while  $^{18}\text{F}$ ,  $^{123}\text{I}$ ,  $^{192}\text{Ir}$  and  $^{153}\text{Sm}$  are occasionally detected or not depending of the WWTP (FANC, 2015). In many instances, the activity levels in the effluents were below the detection limit.

According to these measurements, the current releases do not represent a risk for people or the environment; notwithstanding this, they exemplify that hospital discharges should be the subject of monitoring and regular control. The data gives information not only about activity levels but also about the effluent’s isotopic composition and the release schedule, providing an opportunity for making a pilot study and to identify the data gaps present in assessments of this type.

The present study aligns with the Radioecology ALLIANCE recommendations to EURAMED in the EC Rocc-n-Roll project (Vives i Batlle et al., 2022), which indicated the general research need to (a) identify the behaviour of relevant radionuclides and exposure pathways, (b) improve datasets and assessment methods, identifying the relevant data gaps and (b) provide advice to operators and regulators leading to a future European-level assessment approach. Following these recommendations, the objective of this project, performed within Work Package 3 of the EC project SINFONIA (<https://cordis.europa.eu/project/id/945196>), is to show how to assess the impact of environmental releases of radiopharmaceuticals from hospitals on the public and the environment, using the aforesaid Belgian test case as an example.

Our study involves estimating radionuclide uptake in freshwater wildlife at the outlet of a WWTP in Belgium and resulting uptake and internal/external exposures to aquatic wildlife for a conservative and generic discharge scenario that is used to test the assessment method and to identify knowledge gaps. The data on which this study is based are measurements previously performed at several WWTPs receiving discharges from hospitals across the country. For the human part of the assessment, we consider human ingestion of aquatic biota and drinking of contaminated water as well as external exposures at the riverbank and swimming, including also an indirect mechanism, namely internal doses arising from the consumption of agricultural foodstuffs after irrigation or fertilisation with contaminated sludge.

It is therefore not the purpose to assess the releases of a particular hospital, but to use this semi-realistic scenario to put to the test the different steps of the assessment chain and highlight where more data and process information are required, deriving recommendations for a the development of a more integrated and pan-European assessment system.

## 2. MATERIALS AND METHODS

### 2.1 Case study definition

Our case study is a fictitious situation with a WWTP in Mol releasing into the Molse Nete river in Belgium, but using a generic source term based on the river releases from the hospital of Leuven, given the lack of discharge data for the (smaller) hospitals in the Mol-Geel region of interest. The modelling of the impact of radiopharmaceuticals is based on a series of conservative assumptions, explained in turn below.

The first assumption is selecting the radionuclides at the inlet of WWTP Leuven as a generic test case to provide radionuclide data for the assessment. Our assumption is reasonable because this is the most important centre for cancer research and treatment in Belgium. Additionally, the proportions of this hospital with regard to the number of patients and treatments lead us to presume that the rest of the hospitals in the country could increase their releases in the future up to similar levels, given the growing demand for medical treatments of this nature. The activity concentrations at the inlet of WWTP Leuven are periodic and change over the day, so this source term captures the typical variability in the dilution of the activity concentration, making it an essentially dynamic problem.

Secondly, for the assessment of impact to the environment and members of the public, we made the penalising assumption that the hospital effluents from the decay tanks reaching the WWTP inlet are bypassed directly into the river. This could occur under extraordinary circumstances such as maintenance or expansion of the WWTP, so it is necessary to include it in our (conservative) assessment.

Thirdly, we assume that the aquatic biota and the members of the public are located directly at the outlet of the WWTP where the concentrations are maximal. The released radionuclides would spread downstream the release point, travelling across the river network which has a long hydrological simulation domain, but concentrations and the resulting dose rates would be much lower at increasing distances downstream from the WWTP.

In fourth place, we selected the low-flow year 2018 as reference year because the highest concentration in the river occurs during the periods where the river discharge is very low. In principle, it would be sufficient to just calculate the activity concentration in the river for the driest historical period, but we were also interested to investigate the fluctuations within a year to assess the variability of dose in relation to the accepted limits. Therefore, the release time series were cycled to have a registry for a full year. Using the available hydrometric data, we concluded that the year 2018 was one of the driest in the last decennia, especially in summer, leading to selecting this year as the test case for subsequent study. Specifically, we used the 7-day, 10-year low flow ( $Q_7, 10$ ) statistic as an indicator. The ( $Q_7, 10$ ) is the 7-day minimum flow that is expected to occur every 10 years (Chapra, 1997). The calculation of the ( $Q_7, 10$ ) was done based on the last 35 years of flow registries. Our calculation shows that the summer

of 2018 was one of the driest summers in the last decennia, justifying the selection of 2018 as the representative year for this study. In addition, the number of low flows around the minimum flow observed in 2018 is higher in comparison to other years.

Lastly, we made the conservative assumption for workers of the WWTP in Mol that the plant is actively taking-up radionuclides from the water according to literature-based retention efficiencies, leading to exposures to plant operating and maintenance workers and doses from agricultural application of water and sludge. This is deliberately opposite to the assumption of free release for the non-human biota and members of the public.

The high conservatism of our assumptions means that the results must not be interpreted as an impact assessment of the UZ Leuven hospital as such, which would be much lower than calculated here, but rather as a generic, approximated benchmark simulation which, in so far as possible, is used to understand the assessment chain for radiological discharges from hospitals to rivers, and to give a conservative estimation of the potential impact of similar discharges in the Molse Nete region.

Our model simulations led to the calculation of activity concentrations of  $^{18}\text{F}$ ,  $^{123}\text{I}$ ,  $^{131}\text{I}$ ,  $^{153}\text{Sm}$ ,  $^{99\text{m}}\text{Tc}$  and  $^{201}\text{Tl}$  in 10-minute intervals taking into account their decay half-lives, their distribution between solid and liquid phases, the volumes and activity levels, the high discharge periodicity of the radioactive effluents and the river's flow regime. We refer to a previous report (Fiengo Pérez et al., 2022) for details on the hydrological simulations performed. In short, the model used for the dispersion simulation is DHI MIKE 11-ECO Lab framework. This model solves the full, dynamic, 1-D shallow-water equations in unidirectional form, also called Saint Venant equations (Hervouet, 2007). Direct verification of the model's hydrological predictions across the whole simulation domain could not be fully carried out with the data available to represent a highly complex system, but the model's capacity to simulate a complex river network has been verified separately during an ongoing model evaluation for tritium in collaboration with the IRSN (France) for the Rhône River (Fiengo Pérez et al., 2022). Nevertheless, our predictions of flow rate and activity concentrations in this exercise matched the limited data available.

We also calculated an accidental scenario involving the release into the sewer system of a 1-MBq  $^{131}\text{I}$  therapeutic capsule as used for thyroid cancer treatment. The resulting doses can be scaled up or down to fit a range of possible radionuclide activities.

## **2.2 Basis of the impact assessment approach**

The sequence followed to develop the assessment is as follows:

1. Devising a list of relevant radionuclides and creating a database of radioecological parameters for freshwater wildlife: expected chemical form, decay half-life, distribution coefficient ( $K_d$ ), transfer factor and biological half-life information. We used mostly data from the ERICA assessment tool for wildlife impact assessment (Brown et al., 2008; Brown et al., 2013) and associated data collection

approaches (Beresford et al., 2015b) where data was not directly available, including extrapolation methods to fill in the data gaps.

2. Adaptation of the Dynamic Dose Assessment Tool (D-DAT) model for marine wildlife (Vives Batlle et al., 2008; Vives i Batlle, 2016) to cover the freshwater environment, by re-parameterising the model with information from the aforesaid database and introducing the relevant radionuclides. This task included also the incorporation of a new human exposures post-processor into D-DAT to calculate doses to people arising from the consumption of aquatic wildlife or exposure to the contaminated water.
3. Production of a simple model to calculate doses to waste treatment plant workers, sewer maintenance workers and the public drinking the water and eating from the terrestrial food chain. This model was grounded on a previous example of assessment of liquid pharmaceutical discharges in sewers (McDonnell, 2004; Titley et al., 2000) but with significant methodological and functional differences and customised with the relevant radionuclides and assessment parameters for the Belgian situation.

### 2.3 Database of radioecological parameters

The radionuclide parameters listed in the database cover  $^{18}\text{F}$ ,  $^{89}\text{Zr}$ ,  $^{90}\text{Y}$ ,  $^{99}\text{Mo}$ ,  $^{99\text{m}}\text{Tc}$ ,  $^{123}\text{I}$ ,  $^{131}\text{I}$ ,  $^{131\text{m}}\text{Xe}$ ,  $^{133}\text{Xe}$ ,  $^{153}\text{Sm}$ ,  $^{177}\text{Lu}$ ,  $^{177\text{m}}\text{Lu}$ ,  $^{201}\text{Tl}$ ,  $^{223}\text{Ra}$ ,  $^{225}\text{Ac}$ ,  $^{226}\text{Ra}$  and  $^{227}\text{Th}$ , although in practice this study covers only for  $^{18}\text{F}$ ,  $^{123}\text{I}$ ,  $^{131}\text{I}$ ,  $^{153}\text{Sm}$ ,  $^{99\text{m}}\text{Tc}$  and  $^{201}\text{Tl}$  because these are the only radionuclides detected in the Leuven WWTP. Data for the remaining radionuclides are kept in readiness for future studies.

This database contains the following information: radionuclide chemical form, half-life, the solid-liquid distribution coefficient  $K_d$ , and the concentration factor CF and biological half-lives of elimination  $T_{B1/2}$  for multiple processes. This information, covering general radionuclide information and biological half-lives, is presented in Tables 1 and 2, respectively.

We conducted detailed reviews to obtain much of the data but, when not available, we used a simple analogy with closest chemical element to fill parameter gaps. Since CFs for  $^{99}\text{Mo}$  and  $^{177}\text{Lu}$  could not be found in the ERICA database, we used a conservative value from another transition element for  $^{99}\text{Mo}$  and a lanthanide for  $^{177}\text{Lu}$ : Tc was used as an analogue for Mo as it is the nearest transition metal in terms of closest atomic number.

For lutetium, the situation is more difficult; The ERICA Tool has data for La, Ce and Eu with La and Ce having high  $K_d$ s and Eu behaving more as a soluble element. It is stated that  $K_d$ s for lanthanides vary in the order  $\text{Eu} < \text{Ho} < \text{Gd} < \text{Er} < \text{Dy} < \text{La}$  (Tomczak et al., 2019); clearly it is better to take a high value for Lu from among the lanthanides, which signals that our most appropriate analogue for Lu and Sm radionuclides is Eu. In similar fashion, we used Cl data as an analogue for F, given the closeness of these elements in the periodic table. For the CF and  $K_d$  specifically, additional sources of information and data extrapolation included data from the ongoing new revision of the IAEA SRS-19 report (IAEA,

2001), and other sources describing Tc uptake experiments for crustaceans and molluscs, performed at Oregon State University (Hevland, 1981; McKenzie-Carter, 1985).

The thallium  $K_d$  is a sensitive parameter in our study, given the activities and retention times involved. Here, a single suitable source was found (Seaman and Kaplan, 2010). For the CR data gaps encountered for  $^{201}\text{Tl}$  we used published measurement data (Zitko, 1975) for fish and we used Pb as an analogue for macroalgae. The principal source available for the biological half-lives is the freely available international database of radionuclide biological half-life values developed during the IAEA project MODARIA (<https://www-ns.iaea.org/projects/modaria/modaria2.asp?s=8&l=129>, which includes 1907 entries for 52 elements for terrestrial, freshwater, riparian and marine organisms (Beresford et al., 2015a). Additional biological half-lives were taken from the IAEA INIS database (<https://www.iaea.org/resources/databases/inis>), with some success for direct data for lanthanides and thorium. We also performed data gap extrapolation by finding the nearest radionuclide or biological analogues as described previously (these data are appropriately colour-coded in the database).

In some cases, our scientific judgement indicated that it was more adequate to use information from other sources not linked to the IAEA biological half-life database, and that additional literature was more suitable. Moreover, we used data for carp (*Cyprinus carpio*) and mosquitofish (*Gambusia affinis*) (Blaylock and Frank, 1981). For thorium in fish, we used additional published data (Mahmood et al., 2014).

The extrapolation method indicated above, based on consideration of nearest chemical analogue, has the potential to be improved in future using chemical speciation knowledge. For example, iodate could be used to predict the long-term behaviour of  $^{99}\text{Tc}$ , which is present in the aquatic environment mainly as the pertechnetate ion  $\text{TcO}_4^-$ .

Table 1: Database of radionuclide parameters and related information

RN	Relevance	Chemical (administered)	Chemical form (speciation)		$\lambda$ (d <sup>-1</sup> )	Kd (m <sup>3</sup> kg <sup>-1</sup> )	Concentration ratio (Bq kg <sup>-1</sup> FW per Bq m <sup>-3</sup> )					
			As administered	Environment			Fish	Crust.	Bivalve	Aq. plant	Phytopl.	Zoopl.
<sup>89</sup> Zr	Used in positron emission tomography (PET)	Radiolabeled monoclonal antibodies		Soluble	2.1E-01	1.7E+02	1.3E+00	8.2E-01	8.2E-01	9.7E-02	8.2E-01	1.5E+00
<sup>90</sup> Y	Used in cancer radiotherapy	<sup>90</sup> YCl <sub>3</sub> labelled particles injection	Y <sup>+3</sup> (ionic)	Soluble	2.6E-01	4.0E+00	7.9E-02	2.3E+00	2.3E+00	3.8E-01	2.3E+00	6.9E+00
<sup>99m</sup> Mo	<sup>99m</sup> Tc production	Not administered		Highly soluble	2.5E-01	2.6E-02	9.9E-02	9.9E-02	9.9E-02	9.9E-02	9.9E-02	9.9E-02
<sup>99m</sup> Tc	Nuclear medicine diagnostics	<sup>99m</sup> TcO <sub>4</sub> <sup>-</sup> (VII), other III or IV reduced complexes	<sup>99m</sup> TcO <sub>4</sub> <sup>-</sup>	Highly soluble	2.8E+00	2.6E-02	9.9E-02	9.9E-02	9.9E-02	9.9E-02	9.9E-02	9.9E-02
<sup>131</sup> I	<sup>99</sup> Mo byproduct, thyroid radiotherapy, diagnostic cameras	sodium iodide (Na <sup>131</sup> I) and metaiodobenzylguanidine	I <sup>-</sup>	Moderately insoluble	8.6E-02	1.1E+00	3.1E-01	8.0E-02	8.0E-02	5.3E-02	8.0E-02	5.3E-02
<sup>131m</sup> Xe	By-product of <sup>99</sup> Mo production	Noble gas (not administered)	Free element	Gas	5.9E-02	0.0E+00	0.0E+00	0.0E+00	0.0E+00	0.0E+00	0.0E+00	0.0E+00
<sup>133</sup> Xe	By-product of <sup>99</sup> Mo production	Noble gas (not administered)	Free element	Gas	1.3E-01	0.0E+00	0.0E+00	0.0E+00	0.0E+00	0.0E+00	0.0E+00	0.0E+00
<sup>177</sup> Lu	Radiopharmaceutical precursor used for radiolabelling medicines	<sup>177</sup> LuCl <sub>3</sub> , Lutathera lutetium ( <sup>177</sup> Lu)-oxodotreotide	Akaline, Lu(OH) <sub>3</sub>	Highly soluble	1.0E-01	2.9E+02	6.2E-02	1.6E+00	1.6E+00	2.2E-01	1.6E+00	8.3E+00
<sup>177m</sup> Lu	Production of <sup>177</sup> Lu from <sup>177m</sup> Lu	Not administered	Akaline, Lu(OH) <sub>3</sub>	Highly soluble	4.3E-03	2.9E+02	6.2E-02	1.6E+00	1.6E+00	2.2E-01	1.6E+00	8.3E+00
<sup>223</sup> Ra	Xofigo therapy with <sup>223</sup> Ra to treat bone tumours.	<sup>223</sup> RaCl <sub>2</sub>		Moderately soluble	6.1E-02	8.5E+00	1.0E+00	2.8E-01	5.2E+01	8.7E-01	5.2E+01	5.2E-01
<sup>225</sup> Ac	Targeted $\alpha$ -particle cancer therapy	Free metal or chelating/complexing agents		Highly insoluble	7.0E-02	2.0E+04	1.1E+00	3.4E+01	3.4E+01	4.4E+01	3.4E+01	1.2E+01
<sup>226</sup> Ra	<sup>225</sup> Ac production in LINAC by bombarding <sup>226</sup> Ra	Not administered	Insoluble	Moderately soluble	1.2E-06	8.5E+00	1.0E+00	2.8E-01	5.2E+01	8.7E-01	5.2E+01	5.2E-01
<sup>227</sup> Th	Targeted thorium conjugates (TTC)	Attached to targeting proteins for tumor delivery		Highly insoluble	3.7E-02	2.7E+02	7.2E-01	1.7E+01	1.7E+01	4.4E+01	1.7E+01	1.2E+01
<sup>18</sup> F	Tracer for PET.	NAF and fluorodeoxyglucose	F <sup>-</sup>	F <sup>-</sup> (soluble)	9.1E+00	1.0E-03	1.0E+00	1.0E+00	1.0E+00	2.8E-01	1.0E+00	2.8E-01
<sup>123</sup> I	Single photon emission computed tomography (SPECT)	Supplied as NaI in 0.1 M sodium hydroxide solution	I <sup>-</sup>	Moderately insoluble	1.3E+00	1.1E+00	3.1E-01	8.0E-02	8.0E-02	5.3E-02	8.0E-02	5.3E-02
<sup>153</sup> Sm	Bone cancer palliation	Component of samarium lexicidronam.	Chelated complex	Ca analog – bone-seeker	3.6E-01	2.9E+02	6.2E-02	1.6E+00	1.6E+00	2.2E-01	1.6E+00	8.3E+00
<sup>201</sup> Tl	Myocardial perfusion imaging, SPECT for heart diagnosis	Thallous (I) chloride (TlCl) injection	Tl <sup>+</sup> (ionic)	Soluble. Tl(III) sorbs stronger	2.3E-01	1.7E+00	6.5E-01	9.8E-01	9.8E-01	4.7E-01	9.8E-01	8.6E-01

- IAEA live chart of nuclides (<https://www-nds.iaea.org/relnsd/vcharthtml/VChartHTML.html>)
- Using Tc as an analogue for Mo - nearest transition metal in terms of atomic number.
- Data from new revision of IAEA SRS-19 report (IAEA, 2001).
- Using Eu as an analogue for Lu and Sm as it maximises Kd for the three available candidates (La, Ce and Eu).
- Assumption of Kd = 0 and CR = 0 for noble gases.
- Ac transfer factors from the ERICA Tool (Brown et al., 2016), mostly extrapolated from Pu, Am and Th and some of the CRs are even based on data.
- Y transfer factors from the latest ERICA version, originating from the IAEA wildlife transfer parameter database (<https://www.wildlifetransferdatabase.org/>).
- Primary value from the ERICA tool with or without extrapolation.
- From direct sources describing uptake experiments (Hevland, 1981; McKenzie-Carter, 1985).
- Using Cl as an analogue for F.
- Using Pb as analogue (data from the ERICA Tool).
- Published data on thallium toxicity (Zitko, 1975).

Table 2: Database of biological half-lives). Note the analogies between the following pairs of elements: Ac and Ra, F and I, Sm, Lu and Eu. Values in red are extrapolated from a related species (plant to phytoplankton or crustacean to zooplankton) or radionuclide analogues (Y as analogue for Zr).

Rn	Biological half-life (d) – primary data						Short-term biological half-life with data extrapolation (d)						Long-term biological half-life with data extrapolation (d)					
	Fish	Crust.	Bivalve	Aq. plant	Phytopl.	Zoopl.	Fish	Crust.	Bivalve	Aq. plant	Phytopl.	Zoopl.	Fish	Crust.	Bivalve	Aq. plant	Phytopl.	Zoopl.
<sup>89</sup> Zr				5.2E+00			8.4E+00	1.4E+00	2.0E+00	6.9E-03	6.9E-03	1.4E+00	6.9E+01	8.5E+01	6.9E+01	5.2E+00	2.7E+00	6.2E+01
<sup>90</sup> Y				5.2E+00			8.4E+00	1.4E+00	2.0E+00	6.9E-03	6.9E-03	1.4E+00	6.9E+01	8.5E+01	3.4E+01	5.2E+00	2.7E+00	6.2E+01
<sup>99</sup> Mo	3.4E+00	3.0E+00 (14%) 1.4E+02 (83%)	1.0E+02			3.0E+00 (14%) 1.4E+02 (83%)	8.4E+00	3.0E+00	2.0E+00	6.9E-03	6.9E-03	3.0E+00	3.4E+00	1.4E+02	1.0E+02	3.6E+00	2.7E+00	1.4E+02
<sup>99m</sup> Tc	3.4E+00	3.0E+00 (14%) 1.4E+02 (83%)	1.0E+02			3.0E+00 (14%) 1.4E+02 (83%)	8.4E+00	3.0E+00	2.3E+03	6.9E-03	6.9E-03	3.0E+00	3.4E+00	1.4E+02	1.0E+02	3.6E+00	3.0E+00	1.4E+02
<sup>131</sup> I	3.4E+00	3.0E+00 (14%) 1.4E+02 (83%)	1.0E+02			3.0E+00 (14%) 1.4E+02 (83%)	8.4E+00	3.0E+00	2.3E+03	6.9E-03	6.9E-03	3.0E+00	3.4E+00	1.4E+02	1.0E+02	3.6E+00	3.0E+00	1.4E+02
<sup>131m</sup> Xe	0.0E+00	0.0E+00	0.0E+00	0.0E+00	0.0E+00	0.0E+00	0.0E+00	0.0E+00	0.0E+00	0.0E+00	0.0E+00	0.0E+00	0.0E+00	0.0E+00	0.0E+00	0.0E+00	0.0E+00	0.0E+00
<sup>133</sup> Xe	0.0E+00	0.0E+00	0.0E+00	0.0E+00	0.0E+00	0.0E+00	0.0E+00	0.0E+00	0.0E+00	0.0E+00	0.0E+00	0.0E+00	0.0E+00	0.0E+00	0.0E+00	0.0E+00	0.0E+00	0.0E+00
<sup>177</sup> Lu			2.0E+00 (61%) 3.4E+01 (39%)	2.7E+00	2.7E+00	2.7E+00	8.4E+00	1.4E+00	2.0E+00	6.9E-03	6.9E-03	1.4E+00	6.9E+01	8.5E+01	3.4E+01	2.7E+00	2.7E+00	6.2E+01
<sup>177m</sup> Lu			2.0E+00 (61%) 3.4E+01 (39%)	2.7E+00	2.7E+00	2.7E+00	8.4E+00	1.4E+00	2.0E+00	6.9E-03	6.9E-03	1.4E+00	6.9E+01	8.5E+01	3.4E+01	2.7E+00	2.7E+00	6.2E+01
<sup>223</sup> Ra	1.0E+01 2.7E+02	1.7E-01 4.3E+01	4.0E+03	6.9E-03 3.2E+00	6.9E-03 3.2E+00	3.2E+00 2.5E-01 2.3E+00	1.0E+01	1.7E-01	4.0E+03	6.9E-03	6.9E-03	2.5E-01	2.7E+02	4.3E+01	4.0E+03	3.2E+00	3.2E+00	2.3E+00
<sup>225</sup> Ac							8.4E+00	1.7E-01	4.0E+03	6.9E-03	6.9E-03	2.5E-01	1.6E+02	4.3E+01	4.0E+03	3.2E+00	3.2E+00	2.3E+00
<sup>226</sup> Ra	6.7E+00 4.9E+01	1.7E-01 4.3E+01	4.0E+03	6.9E-03 3.2E+00	6.9E-03 3.2E+00	2.5E-01 2.3E+00	6.7E+00	1.7E-01	4.0E+03	6.9E-03	6.9E-03	2.5E-01	5.0E+01	4.3E+01	4.0E+03	3.2E+00	3.2E+00	2.3E+00
<sup>227</sup> Th	8.8E-01						8.4E+00	1.7E-01	4.0E+03	6.9E-03	6.9E-03	2.5E-01	8.8E-01	4.3E+01	4.0E+03	3.2E+00	3.2E+00	2.3E+00
<sup>18</sup> F							8.4E+00	3.0E+00	2.3E+03	6.9E-03	6.9E-03	3.0E+00	3.4E+00	1.4E+02	1.0E+02	3.2E+00	3.0E+00	1.4E+02
<sup>123</sup> I	0.0E+00	0.0E+00	0.0E+00			0.0E+00	8.4E+00	3.0E+00	2.3E+03	6.9E-03	6.9E-03	3.0E+00	3.4E+00	1.4E+02	1.0E+02	3.2E+00	3.0E+00	1.4E+02
<sup>153</sup> Sm			2.0E+00 (61%) 3.4E+01 (39%)	2.7E+00	2.7E+00	2.7E+00	8.4E+00	1.4E+00	2.3E+03	6.9E-03	6.9E-03	1.4E+00	6.9E+01	8.5E+01	3.4E+01	2.7E+00	2.7E+00	6.2E+01
<sup>201</sup> Tl							8.4E+00	1.4E+00	2.3E+03	6.9E-03	6.9E-03	1.4E+00	6.9E+01	8.5E+01	2.4E+03	3.4E+00	3.1E+00	6.2E+01

- From direct sources describing uptake experiments (Hevland, 1981; McKenzie-Carter, 1985).
- Using Tc as an analogue for Mo - nearest transition metal in terms of atomic number.
- Published data for carp (*Cyprinus carpio*) and mosquitofish (*Gambusia affinis*) (Blaylock and Frank, 1981).
- Assumption of zero for noble gases.
- Taking Ce as analogue and using the MODARIA WG8 Biological half-life database (<http://dx.doi.org/10.1016/j.jenvrad.2015.08.018>).
- Direct average from MODARIA WG8 Biological half-life database (<http://dx.doi.org/10.1016/j.jenvrad.2015.08.018>).
- Published data (Mahmood et al., 2014).
- Published data (Seaman and Kaplan, 2010).

## 2.4 Adaptation of the D-DAT model for freshwater assessments

### 2.4.1 Brief description of the D-DAT model

The D-DAT assessment model (Vives i Batlle et al., 2008) calculates aquatic wildlife radionuclide concentrations (fish, crustaceans, molluscs, macroalgae, phytoplankton and zooplankton) and the resulting dose rates to biota using time series of contaminated water concentrations (measured or modelled) as input. In addition, the model contains a sediment sub-model that considers suspended particulates, molecular diffusion, pore water mixing and bioturbation, in order to dynamically calculate sediment activity concentrations and therefore external dose rates to wildlife arising from sediment exposure. This model has been successfully applied to Fukushima studies (Vives i Batlle et al., 2018) and was further developed into an advanced version which was the offspring of the Euratom project COMET (Vives Batlle, 2013; Vives i Batlle et al., 2018). That model implements a dual  $T_{B1/2}$  approach, requiring three compartments: water ( $A_W$ ), as well as a fast ( $A_{OF}$ ) and slow ( $A_{OS}$ ) organism, linked to fast and slow routes of uptake and release, respectively:

$$\frac{dA_W}{dt} = -(K_{Wf} + K_{WS} + \lambda)A_W + \frac{m}{V}(K_{OF}A_{OF} + K_{OS}A_{OS})$$

$$\frac{dA_{Of}}{dt} = K_{WF} \frac{m}{V} A_W - (K_{Of} + \lambda)A_{Of}; \frac{dA_{Os}}{dt} = K_{WS} \frac{m}{V} A_W - (K_{OS} + \lambda)A_{Os}$$

Where  $K_{ij}$  are the rate constants governing transfer from compartment  $i$  to compartment  $j$  (where  $i$  and  $j$  symbolise the water, organism-fast and organism-slow retention phases  $W$ ,  $OF$  or  $OS$ );  $\lambda$  is the radionuclide decay constant;  $m$  is the mass of the organism;  $V$  is the volume of the water compartment with  $K_{Of} = \frac{\ln(2)}{T_{B1/2}^F}$  and  $K_{Os} = \frac{\ln(2)}{T_{B1/2}^S}$  (where  $T_{B1/2}^F$  and  $T_{B1/2}^S$  are the two “fast” and “slow” biological half-lives of elimination which can, in the general case, be present simultaneously). The exchange of radionuclides between water and sediment is represented by the dynamic coupling of the above model with a four-compartment (water and 3 layers of sediment) linear, first order kinetic exchange model (Lepicard et al., 2004; Lepicard et al., 1998; Simmonds et al., 2004) which includes the processes of particle scavenging, molecular diffusion, particle mixing, pore water mixing and sedimentation.

To calculate internal and external dose rates to the wildlife for the various radionuclides, activity concentrations (sum of the “slow” and the “fast” component) are multiplied by the dose coefficients ( $\mu\text{Gy h}^{-1}$  per  $\text{Bq kg}^{-1}$ ), or DCs, for the required organism from ICRP Publication 136 (ICRP, 2017). External dose rates are calculated similarly by using external exposure DCs and purposely-defined occupancy factors that account for hybrid exposure from both water and sediment.

D-DAT is currently implemented in the ModelMaker<sup>®</sup> 4 software (Adamatzky, 2001; Citra, 1997; Rigas, 2000) and, in this form, it has had a very successful track record of application to a variety of environmental situations involving non-continuous discharges of radionuclides in the marine

environment, as well as having been successfully tested in inter-comparisons with other dynamic models (Vives Batlle et al., 2008; Vives i Batlle, 2016; Vives i Batlle et al., 2016).

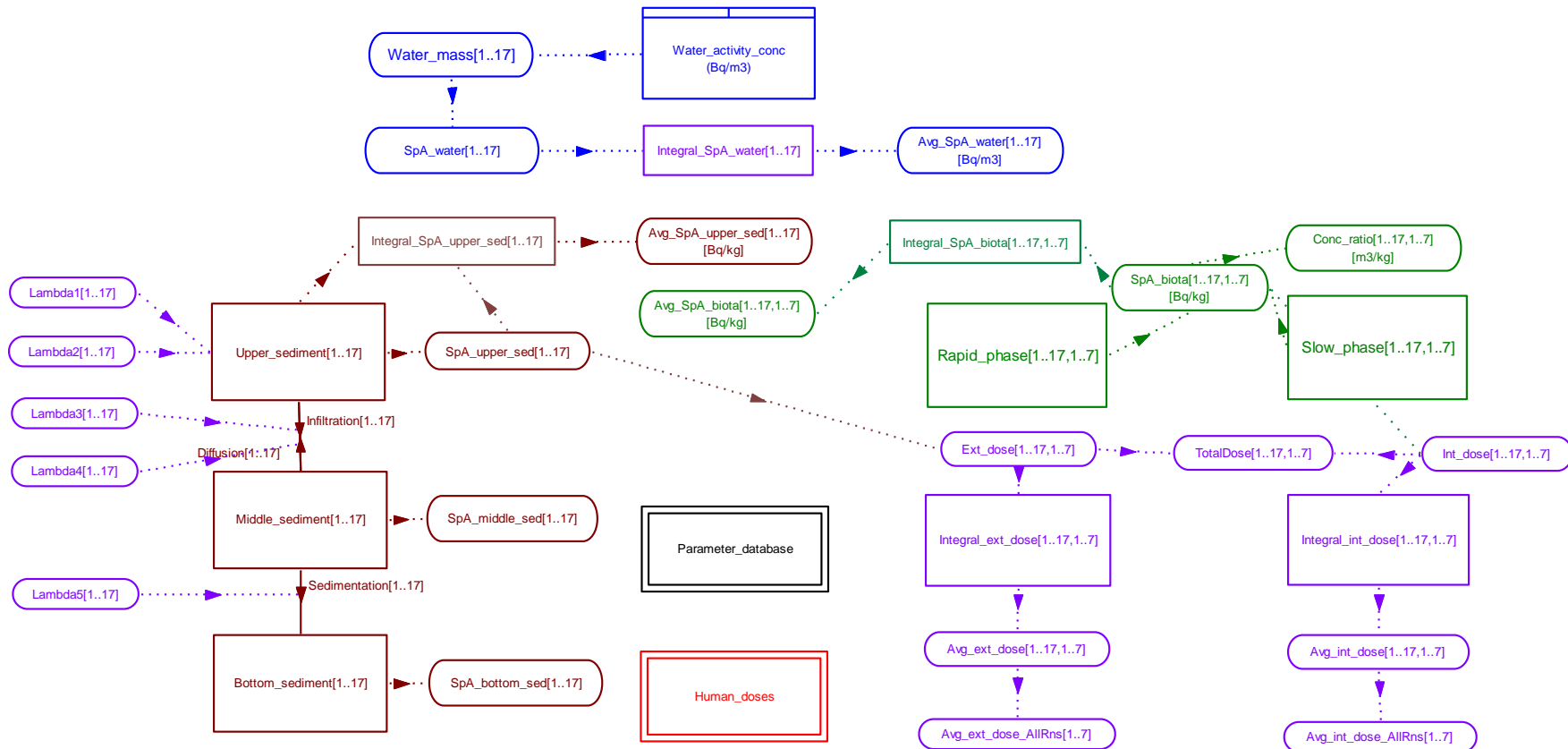
The ability of D-DAT to balance incoming activity concentrations of radionuclides in water at the wildlife receptor location, combined with the explicit modelling of the role of sediments as a potential dose-giving reservoir of radionuclides, means that D-DAT is eminently suitable for adaptation to carry out the present study for the freshwater environment, extending the original radionuclide set (the model was originally designed for the long-lived radionuclides  $^{90}\text{Sr}$ ,  $^{99}\text{Tc}$ ,  $^{129,131}\text{I}$ ,  $^{134,1237}\text{Cs}$ ,  $^{239,240}\text{Pu}$ ,  $^{241}\text{Am}$  and  $^{236}\text{U}$ ) to the short-lived medical radionuclides considered in medical releases.

## 2.5 Adaptation of D-DAT to medical radionuclides in freshwater

The D-DAT model performs simultaneous calculations for a suite of radionuclides and organisms thanks to a very compact form of the model's differential equations, which are indexed as a two-dimensional array, with the first index  $i$  signifying the radionuclide and the index  $j$  signifying the wildlife group. The model's parameters are also stored in multidimensional array format. Therefore, the first step in the adaptation of D-DAT for freshwater was the re-indexing of all the compartments and fluxes of the model to accommodate the new radionuclides, as shown in Fig. 1.

A significant improvement to the original D-DAT model was adding a human dosimetry post-processing module. This module is capable of calculating as function of time: (a) time-dependent aquatic food ingestion doses, and associated annually-averaged ingestion doses to all age groups, foods and radionuclides; (b) time-dependent and annually-averaged water ingestion dose rates and (c) time-dependent, and also annually averaged, external dose rates from exposure to both sediment (riverbank) and water (swimming) exposure to all radionuclides.

Internal dose rates are calculated conventionally by multiplying the activity concentration in the wildlife used as food ( $\text{Bq kg}^{-1}$ ) per the ingestion rate ( $\text{kg y}^{-1}$ ), the dose per unit via intake via ingestion ( $\text{Sv Bq}^{-1}$ ) from ICRP Publications 72 and 119 (ICRP, 1996, 2012) and the fraction of food that is obtained locally. For external exposures, the model uses the committed effective doses to 70 years of age per unit time and deposited activity of radionuclide on the riverbank in  $\text{Sv Bq}^{-1} \text{ s}^{-1} \text{ m}^2$  (Eckerman and Ryman, 1993), maximally assumed to be as contaminated as sediment, so as to estimate doses for riverbank exposure to members of the public. We deduced the modelled activity per unit area of riverbank soil ( $\text{Bq m}^{-2}$ ) by multiplying the activity concentration by a 0.3-m active soil contamination depth and by the external dose coefficient and per the number of seconds in a year, with further application of a factor of 0.5 to account for the geometry of the source/target distribution on the riverbank and application of the occupancy factor, giving the external exposure dose rate.



1

2 Figure 1: Representation of the new version of D-DAT for freshwater in ModelMaker 4, showing integrating compartments (rectangles), embedded sub-models  
 3 (double rectangles), variables (rounded rectangles) and influences (dotted arrows). The compartments are indexed as two-dimensional arrays as follows. The  
 4 sub-indices  $i = 1$  to 17 represent the radionuclides  $^{89}\text{Zr}$ ,  $^{90}\text{Y}$ ,  $^{99}\text{Mo}$ ,  $^{99\text{m}}\text{Tc}$ ,  $^{131}\text{I}$ ,  $^{131\text{m}}\text{Xe}$ ,  $^{133}\text{Xe}$ ,  $^{177}\text{Lu}$ ,  $^{177\text{m}}\text{Lu}$ ,  $^{223}\text{Ra}$ ,  $^{225}\text{Ac}$ ,  $^{226}\text{Ra}$ ,  $^{227}\text{Th}$ ,  $^{18}\text{F}$ ,  $^{123}\text{I}$ ,  $^{153}\text{Sm}$  and  $^{201}\text{Tl}$ ,  
 5 respectively. The sub-indices  $j = 1$  to 7 represent the freshwater biota organisms Pelagic Fish, Benthic Fish, Crustacean, Mollusc, Macroalgae, Phytoplankton  
 6 and Zooplankton, respectively.

7 The model uses an average individual shore occupancy rate of around 500 h per year (occupancy fraction  
8 of  $5.7 \times 10^{-2}$ ), deemed to be sufficiently conservative. Any additional dose from irradiation of the skin  
9 due to direct contact with sediment is not included in the methodology because it is not a major  
10 contributor to the overall doses.

11 The above extensions to the model required the addition of new parameters, namely human food  
12 ingestion and water drinking rates for infant, child and adult, occupancy factors for external exposure to  
13 shoreline sediments, fraction of locally produced food, internal dose coefficients for ingestion and  
14 external dose coefficient for ground surface and water immersion.

15 The model was verified to check that all equations were correct. In particular, the complex input data  
16 structure was scrutinised to ensure that the input parameters are read correctly, and the integration  
17 algorithm was optimised, given the large number of data points of the input file provided by the  
18 hydrological simulations, which give a full year of water activity concentration data at 10-minute  
19 intervals. In the end, the Euler solving method was selected, with a random seed of one and running  
20 with a fixed step of  $5.2 \times 10^4$  user-defined output points.

## 21 **2.6 Excel dose calculator for water treatment plant workers, sewer maintenance** 22 **workers and the public**

23 The initial starting point was the UK NRPB methodology for the radiological assessment of liquid  
24 pharmaceutical discharges in sewers (McDonnell, 2004; Titley et al., 2000), which has now been  
25 developed into the IRAT-2 approach ([https://www.gov.uk/government/publications/initial-radiological-](https://www.gov.uk/government/publications/initial-radiological-assessment-methodology)  
26 [assessment-methodology](https://www.gov.uk/government/publications/initial-radiological-assessment-methodology)). We used a modified and simplified approach to suit the methodological  
27 needs of the Belgian situation, and we implemented the resulting equations in an Excel calculator to  
28 perform dose screening to workers and the public drinking the water and eating from the terrestrial  
29 foodchain, based on monthly concentration averages.

30 Calculations are based on the assumption of steady state conditions, where discharges are assumed to  
31 take place at a uniform rate and there is little change in the flow rates downstream of the discharge point.  
32 This is because there is no simple equivalent of the D-DAT model in the form of a tool to calculate  
33 dynamically doses from short-lived radionuclides to humans. This would involve use of complex  
34 pharmacokinetic models, with an inevitable lack of associated parameter data for the radionuclides  
35 involved. In general, complex models comprise large amount of parameters and variables that are  
36 difficult to obtain. Our simplified approach is appropriate for screening assessments, requires relatively  
37 few parameters and is adequately conservative.

38 The calculator includes the following radionuclides:  $^{18}\text{F}$ ,  $^{89}\text{Zr}$ ,  $^{90}\text{Y}$ ,  $^{99}\text{Mo}$ ,  $^{99\text{m}}\text{Tc}$ ,  $^{123}\text{I}$ ,  $^{131}\text{I}$ ,  $^{131\text{m}}\text{Xe}$ ,  $^{133}\text{Xe}$ ,  
39  $^{153}\text{Sm}$ ,  $^{177}\text{Lu}$ ,  $^{177\text{m}}\text{Lu}$ ,  $^{201}\text{Tl}$ ,  $^{223}\text{Ra}$ ,  $^{225}\text{Ac}$ ,  $^{226}\text{Ra}$  and  $^{227}\text{Th}$ . However, we used only  $^{18}\text{F}$ ,  $^{123}\text{I}$ ,  $^{131}\text{I}$ ,  $^{153}\text{Sm}$ ,  
40  $^{99\text{m}}\text{Tc}$  and  $^{201}\text{Tl}$  as these are the only radionuclides for which underwater radioactivity measurements  
41 (gamma spectrometry) were provided by the authorities.

42 Using as input annual discharges (calculated as average annual concentration in Bq m<sup>-3</sup> multiplied by  
43 the flow rate in m<sup>3</sup> y<sup>-1</sup>), our model calculates activity concentrations in the different waste streams at the  
44 plant, namely effluent, a blocked sewer and sludge, whereupon doses to general and maintenance plant  
45 workers could be calculated. This tool also calculates dose rates for the most exposed members of the  
46 public: consumers of locally caught fish, external exposure from frequenting the riverbank, direct  
47 drinking of river water, abstraction of river water for irrigation or drinking water and use of sludge as  
48 fertiliser for agricultural processes. However, it does so assuming average concentrations in water,  
49 thereby making a conservative estimation, whereas the D-DAT model is more appropriate to make a  
50 more detailed, dynamic calculation of doses to public and the environment – so exposes to the public  
51 can in effect be compared here for different modelling assumptions.

### 52 **2.6.1 Dosimetry tool description**

53 The tool as developed has the following calculation worksheets: general assessment parameters, basic  
54 radionuclide data, source term fractions, calculation of dose rates and additional worksheets for transfer  
55 factors, dose factors and assessment assumptions. The general assessment parameters worksheet  
56 contains the required parameter data for the assessment: disposal pathway parameters, data for  
57 assessment of exposure of sewer workers, data used for terrestrial food chain calculations, data used for  
58 soil hydrology calculations and habit data and other parameters for public exposure. Element  
59 independent parameters were chosen specific for the Belgian dataset from the Category A Waste  
60 Disposal project (Sweeck, 2018) or (when not available) literature values (McDonnell, 2004; Titley et  
61 al., 2000) and/or plain expert judgement.

62 The basic radionuclide data parameters worksheet contains radionuclide half-lives, external dose  
63 coefficients for ground surface and water immersion and internal dose coefficients for ingestion and  
64 inhalation for their stated lung classes. The source term fractions worksheet contains an estimation of  
65 the source term and fractions appearing in sewage, leading to estimation of the average radionuclide  
66 concentrations serving as source term for the different assessment locations of interest: blocked sewer  
67 scenario, plant water streams, sludge, the river ecosystem at the plant's outlet and the use of river water  
68 for irrigation and drinking.

69 The calculation of dose rates worksheet contains the main calculation block, with embedded equations  
70 to calculate dose rates to sewer maintenance workers, general workers at the sewage works, dose rates  
71 for the freshwater pathways and dose rates arising from use of river water for irrigation of farmland and  
72 use of sewage sludge in agriculture, as detailed in the sub-sections below. Additional worksheets detail  
73 the transfer and dosimetry factors used in this model for information and data sourcing purposes.

#### 74 *2.6.1.1 Calculation of activity concentrations in blocked sewer and the river*

75 The mean cumulative discharge over a month in Bq,  $A_M$  [Bq] is the main input to the model. We assume  
76 that 100% of the radionuclides discharged from the hospital reach the treatment plant, which is a

77 conservative assumption but one that allows us to obviate site-specific river dispersion modelling  
 78 calculations between the hospital and the plant in favour of a more generic type of screening  
 79 methodology, especially in the present case in which (as will be seen below) the radiological impact,  
 80 even with this assumption, is not significant.

81 It is assumed that the plant has a certain flow of water going through it,  $\phi_{\text{WWTP}}$ , which is less than the  
 82 total flow of the river - the water going through the plant is in fact 1.1% of the total river flow, if we  
 83 assume a typical throughput of 1000 m<sup>3</sup> per day in a river of mean flow of 1.0247 m<sup>3</sup> s<sup>-1</sup> as is typical of  
 84 the Molsė Nete river.

85 The apportioning of the incoming (average) radionuclide concentration [Bq m<sup>-3</sup>] between the various  
 86 compartments is as follows. For a blocked sewer, it is assumed that 1 month-worth of discharges are  
 87 trapped in a pipe blockage, as previously espoused elsewhere (McDonnell, 2004). We take the following  
 88 equation:

$$89 \quad C_{\text{blocked sewer}}[\text{Bq m}^{-3}] = \frac{A_M[\text{Bq}]}{V_{\text{blockage}}[\text{m}^3]} \times \frac{1}{\lambda T} \times f_{\text{blocked drain}}$$

90 Where  $\lambda$  is the decay constant,  $T = 30$  days (the factor  $\frac{1}{\lambda T}$  is the result of averaging  $e^{-\lambda t}$  between 0 and  $T$   
 91 to correct for ongoing decay during the 30 days, assuming that  $\lambda T \gg 1$ :  
 92  $A_{\text{avg}} = \frac{1}{T} \int_0^T A_0 e^{-\lambda t} dt = \frac{A_0}{\lambda T} (1 - e^{-\lambda T}) \approx \frac{A_0}{\lambda T}$ . Moreover,  $f_{\text{blocked drain}}$  is the percentage of activity  
 93 ending in the blockage divided by 100. In other words, the model assumes that a single month's  
 94 discharge is contained in a small volume (2 m<sup>3</sup>) of sewage at a point where the drains have been blocked,  
 95 with workers operating in the vicinity, whilst undergoing decay. The volume estimation is a best  
 96 judgement assumption (Titley et al., 2000).

97 For the plant water streams, we simply consider:

$$98 \quad C_{\text{stream}}[\text{Bq m}^{-3}] = \frac{12A_M/s_y[\text{Bq y}^{-1}]}{\phi[\text{m}^3\text{y}^{-1}]} \times f_{\text{reaching WWTP}}$$

99 Where  $12A_M/s_y$  is simply the average annual discharge rate in Bq s<sup>-1</sup> ( $A_M$  is the monthly discharge and  
 100  $s_y$  is the number of seconds in a year). Therefore, for the sludge:

$$101 \quad C_{\text{sludge}}[\text{Bq m}^{-3}] = \frac{12A_M/s_y[\text{Bq y}^{-1}]}{\phi[\text{m}^3\text{y}^{-1}] \times r_s[-]} \times f_{\text{in sludge}}$$

102 Where  $r_s$  is the annual rate of sludge production to incoming sewage = sludge yearly production rate [m<sup>3</sup>  
 103 y<sup>-1</sup>] per unit of total incoming sewage flow rate [m<sup>3</sup> y<sup>-1</sup>].

104 For the aquatic pathways, the average activity concentration in river water after release is:

$$105 \quad C_{\text{RW}}[\text{Bq m}^{-3}] = \frac{12A_M/s_y[\text{Bq y}^{-1}]}{\phi_{\text{river}}[\text{m}^3\text{y}^{-1}]} \times (1 - \epsilon)$$

106 Where  $\varepsilon$  is the treatment plant's removal efficiency. There are three cases of river flow rate that in our  
 107 calculations are assumed to have the same water concentrations: Water for fish and the calculation of  
 108 the various external exposure pathways such as irrigation and public drinking water supply. Different  
 109 values for these pathways could be introduced if the need arises. It is assumed here that the measured  
 110 activity concentrations supplied to us by the authorities, being so close to the plant, reflect the  
 111 concentration of the undiluted effluent (a conservative assumption).

112 Note that an improvement to this methodology would be to introduce decay terms to account for the  
 113 time delay in the sewage plant. Decay during transit is ignored in this study because the dose rates are  
 114 so low that it does not seem necessary to undergo the complication to calculate to that level of detail.  
 115 Indicative delays that could be used are 0.5 day for milk consumption, 182 days for root vegetables and  
 116 7 days for all other foodstuffs (Titley et al., 2000).

### 117 2.6.1.2 Calculation of concentrations for the irrigation and sludge fertiliser pathways

118 For the irrigation pathway, the starting point is the radionuclide concentration in water  $C_{RW}$  [Bq m<sup>-3</sup>],  
 119 the irrigation water flux  $\phi_W$  [m<sup>3</sup> m<sup>-2</sup> s<sup>-1</sup>], the active depth of contamination (average root soil depth for  
 120 food vegetables)  $d$  [m] and the surface area of the soil =  $S$  [m<sup>2</sup>]. The amount of water infiltrating in the  
 121 soil per unit time is given by the infiltration equation, which takes into account the (higher) pore water  
 122 velocity ( $v_p = v/\theta$  where  $\theta$  is the volumetric water content of the soil) compared with the irrigation water  
 123 fall-in rate  $v$ :  $\frac{dV}{dt} = \frac{\phi_W S}{\theta}$  [m<sup>3</sup> s<sup>-1</sup>]. The rate of change of radionuclide in soil,  $C_{soil}$  [Bq] due to infiltration  
 124 is  $\left(\frac{dC}{dt}\right)_{inf} = C_{RW} \frac{dV}{dt} = \frac{C_{RW} \phi_W S}{\theta} R$  [Bq s<sup>-1</sup>]. Here,  $R = \left[1 + \frac{\rho K_d}{\theta}\right]^{-1} = \left[1 + \frac{\rho_p(1-\varepsilon)K_d}{\theta}\right]^{-1}$  is the  
 125 retardation factor, introduced to consider that the radionuclide may be infiltrating at a lower velocity  
 126 than the water, due to sorption processes as the dissolved radionuclide migrates downwards across the  
 127 soil column. The additional parameters in this equation are the soil/water distribution coefficient  $K_d$  [m<sup>3</sup>  
 128 kg<sup>-1</sup>] and the volumetric water content  $\theta$  [-]. The porosity can be expressed as  $\varepsilon = 1 - \frac{\rho}{\rho_0}$  where  $\rho$  is the  
 129 bulk density of the soil and  $\rho_p$  is the (higher) particle density (both in kg m<sup>-3</sup>).

130 Since the radionuclide is fast decaying, at equilibrium, infiltration balances the loss due to decay which,  
 131 according to the definition of activity, is proportional to the decay constant:  $\left(\frac{dC}{dt}\right)_{decay} = \lambda C_{soil} S d$  [Bq  
 132 s<sup>-1</sup>]. Here,  $C_{PW}$  is the activity concentration in soil pore water [Bq m<sup>-3</sup>],  $S$  is the surface area and  $d$  is the  
 133 active depth of the contamination. Therefore,  $\left(\frac{dC}{dt}\right)_{inf} = \left(\frac{dC}{dt}\right)_{decay} \Rightarrow \frac{C_{RW} \phi_W S}{\theta} R = \lambda C_{PW} S d$ . Hence,  
 134 we arrive at  $C_{PW} = \frac{1}{\theta + \rho K_d} \left(\frac{C_{RW} \phi_W}{\lambda d}\right)$ .

135 The concentration in soil under conditions of equilibrium can be obtained as  $C_{soil} = C_{PW} K_d$ , and the  
 136 concentration in the vegetables is obtained using by further multiplication by the concentration ratio CF  
 137 [m<sup>3</sup> kg<sup>-1</sup>]:  $C_{veg} = C_{soil} CF = C_{PW} K_d CF$ . Thus, the food concentration is  $C_{veg} = \frac{1}{\theta + \rho K_d} \left(\frac{C_{RW} \phi_W}{\lambda d}\right) K_d CF$ ,

138 so we finally obtain a food activity per unit deposited activity ratio  $R$  [Bq/kg per 1 Bq/m<sup>2</sup> per second]

139 of  $R = \frac{C_{veg}}{C_{RW}\phi_W} = \frac{1}{\theta + \rho K_d} \left( \frac{K_d CF}{\lambda d} \right)$ .

140 In this project, we used the following element-independent reference biosphere parameters as input for  
 141 the equations, consistent with the near-surface disposal project for category A waste at Dessel, Belgium  
 142 (Sweeck, 2018): Volumetric water content  $\theta = 0.32$  (general case); average root soil depth  $d = 0.3$  m;  
 143 soil bulk density  $\rho = 1350$  kg m<sup>-3</sup>, soil particle density  $\rho_p = 2650$  kg m<sup>-3</sup> and thus a porosity  $1 - \frac{\rho}{\rho_p} =$   
 144 0.491.

145 The soil activity per unit deposition arising from a concentration in sludge  $C_{sl}$  [Bq kg<sup>-1</sup>], which is being  
 146 applied to farmland at a rate  $\phi_{sl}$  [kg m<sup>-2</sup> s], is calculated as follows. The rate of change of radionuclide  
 147 activity in soil,  $A_{soil}$  [Bq] due to sludge deposition is:  $\frac{dA_{soil}}{dt} = C_{sl}\phi_{sl}S$  [Bq s<sup>-1</sup>], where  $S$  is the surface  
 148 area of the soil. Here again we assume that influx is cancelled by decay, and therefore  $C_{sl}\phi_{sl}S =$   
 149  $\lambda C_{soil}\rho_{soil}Sd \Rightarrow C_{soil} = \frac{C_{sl}\phi_{sl}}{\lambda d\rho_{soil}}$  (here, the term  $C_{soil}\rho_{soil}Sd$  is the activity concentration in soil  
 150 multiplied by the mass of the soil, to convert it to units of absolute activity). From here we can define  
 151 a convenient soil concentration per unit deposition ratio  $CPUD_{soil} = \frac{C_{soil}}{C_{sl}\phi_{sl}} = \frac{1}{\lambda d\rho_{soil}}$  [Bq kg<sup>-1</sup> per unit  
 152 Bq m<sup>-2</sup> s<sup>-1</sup>], which can be used for the calculation of irrigation dose rates, as shown below.

### 153 2.6.2 Calculation of dose rates to WWTP maintenance and sewage workers

154 In order to obtain dose rates, one multiplies the radionuclide concentration by the dose coefficient for  
 155 internal exposure via inhalation or ingestion (internal dose rate) or by the dose coefficient exposure to  
 156 ground surface or immersion (external dose rate), and by additional factors as described in turn below.

157 For accidental ingestion of sludge, one must consider the radionuclide concentration in a blocked sewer  
 158 for maintenance workers, or the average of concentration into sewage works + in sludge for regular  
 159 workers [Bq m<sup>-3</sup>]. For the latter case, is assumed that workers spend 50% of their yearly working time  
 160 in each operation. The pertinent activity concentration in sludge [Bq m<sup>-3</sup>] is then divided by the density  
 161 (approximated by the density of water) to convert the concentration to units of Bq kg<sup>-1</sup>. Then, the result  
 162 is multiplied by the ingestion rate [kg h<sup>-1</sup>], the fractional occupancy  $f_{occ}^{worker}$  for the relevant type of  
 163 worker [h y<sup>-1</sup>] and the internal dose coefficient via ingestion  $DC_{ing}$  [Sv Bq<sup>-1</sup>], leading to:

164 
$$H_{ing} = \frac{C[\text{Bq m}^{-3}]}{\rho[\text{kg m}^{-3}]} \times DC_{ing}[\text{Sv Bq}^{-1}] \times I_R[\text{kg h}^{-1}] \times f_{occ}[\text{h y}^{-1}]$$

165 For inhalation, the approach used here takes the activity concentration [Bq m<sup>-3</sup>] (concentration in  
 166 untreated sewage/sludge for regular workers – assumed to spent 50% of time in each operation) and  
 167 divides it by the water density to convert the concentration to units of Bq kg<sup>-1</sup> of sludge. This is then  
 168 multiplied by the airborne particulate matter concentration  $\gamma_p$  [kg m<sup>-3</sup>] assuming conservatively that these  
 169 particles become inhaled, giving Bq in the particles per unit volume of air. This is then multiplied by

170 the inhalation rate  $B_R$  [ $m^3 h^{-1}$ ], the fractional occupancy for the relevant type of worker [ $h y^{-1}$ ] and the  
 171 internal dose coefficient via inhalation  $DC_{inh}$  [ $Sv Bq^{-1}$ ], leading to the following equation:

$$172 \quad H_{inh} = \frac{C[Bq m^{-3}]}{\rho[kg m^{-3}]} \times \gamma_p[kg m^{-3}] \times DC_{inh}[Sv Bq^{-1}] \times B_R[m^3 h^{-1}] \times f_{occ}^{worker}[h y^{-1}]$$

173 For external gamma exposure, the dose rate is proportional to the surface density of contamination [ $Bq$   
 174  $m^{-2}$ ]. The dose rate derives from the activity concentration [ $Bq m^{-3}$ ] (in a blocked sewer for maintenance  
 175 workers, and mean of plant water and sludge for regular workers – which assumes 50% of time spent in  
 176 each operation) multiplied by the contamination active depth in the WWTP [ $m$ ], assumed here to be 5  
 177 cm, the occupancy fraction for the worker's task [ $h y^{-1}$ ], the external dose coefficient [ $Sv m^2 s^{-1} Bq^{-1}$ ]  
 178 and time units conversions:

$$179 \quad H_{ext} = DC_{ext}[Sv m^2 s^{-1} Bq^{-1}] \times C[Bq m^{-3}] \times d[m] \times f_{occ}^{worker}[h y^{-1}] \times y_h[y h^{-1}] \times s_y[s y^{-1}]$$

180 Where  $y_h$  and  $s_y$  are the unit conversion factors for hours in a year and seconds in a year.

### 181 2.6.3 Calculation of dose rates to the public for the freshwater pathways

182 In this case, it is necessary to calculate first the river input rate data as shown previously (Fiengo Pérez  
 183 et al., 2022):  $I_{river}[MBq y^{-1}] = C_{river}^{avg}[Bq m^{-3}] \times \varphi_{river}[m^3 s^{-1}] \times s_y[s y^{-1}] \times 10^{-6}$ . The external  
 184 gamma dose rate for riverbank occupancy assumes that the riverbank concentration is the riverbed  
 185 concentration, obtained by multiplication of the average water concentration by the  $K_d$ . The fraction  
 186  $\frac{1}{1+S_{susp}K_d}$  is a factor used to take water filtration into account:

$$187 \quad H_{ext}[Sv y^{-1}] = \frac{1}{1+S_{susp}K_d} C_{river}^{avg}[Bq m^{-3}] \times K_d[m^3 kg^{-1}] \times f_{occ}^{riverbank}[h y^{-1}] \times$$

$$188 \quad DC_{groundsurf}^{ext}[Sv Bq^{-1} s^{-1} m^2] \times d[m] \times \rho_{soil}^{bulk}[kg m^{-3}] \times y_h[y h^{-1}] \times s_y[s y^{-1}].$$

189 The ingestion dose rate arising from fish consumption is as follows:

$$190 \quad H_{ing}^{fish}[Sv y^{-1}] = \frac{CR_{fish}[kg kg^{-1}]}{\rho_w[kg m^{-3}]} \times \frac{C_{river}^{avg}[Bq m^{-3}]}{1+S_{susp}K_d} \times I_r^{fish}[kg y^{-1}] \times DC_{ing}[Sv Bq^{-1}]$$

191 In addition, for the ingestion of drinking water and unfiltered river water:

$$192 \quad H_{ing}^{drwater}[Sv y^{-1}] = \frac{C_{river}^{avg}[Bq m^{-3}]}{1+S_{susp}K_d} \times I_r^{drwater}[m^3 y^{-1}] \times DC_{ing}[Sv Bq^{-1}]$$

$$193 \quad H_{ing}^{unfwater}[Sv y^{-1}] = C_{river}^{avg}[Bq m^{-3}] \times I_r^{drwater}[m^3 y^{-1}] \times DC_{ing}[Sv Bq^{-1}]$$

### 194 2.6.4 Calculation of dose rates to the public arising from the agricultural use of sludge

195 As seen above,  $C_{soil}[Bq kg^{-1}] = CPUD_{soil}[m^2 s kg^{-1}] \times C_{sl}[Bq kg^{-1}] \times \phi_{sl}[kg m^{-2} s^{-1}]$ . This can  
 196 be converted to external dose rate (internal exposure is negligible) by means of the following equation:

$$H_{ext} = DC_{ext}[\text{Sv m}^2\text{s}^{-1}\text{Bq}^{-1}] \times C_{soil}[\text{Bq kg}^{-1}] \times \rho[\text{kg m}^{-3}] \times d[\text{m}] \times f_{occ}^{farmland}[\text{h y}^{-1}]$$

$$\times y_h[\text{y h}^{-1}] \times s_y[\text{s y}^{-1}]$$

### 3. RESULTS AND DISCUSSION

#### 3.1 Routine release scenario

##### 3.1.1 Activity concentrations in water, sediment and the wildlife

Figure 2 gives the activity concentrations for the 6 radionuclides considered in the Molsse Nete river at the outlet of the Mol WWTP as modelled by us (Fiengo Pérez et al., 2022), and the resulting activity concentration (calculated dynamically using the D-DAT model) in the upper layer of the riverbed sediment (assumed to be 5-cm). As stated previously, levels in river water assume extraordinary circumstances such as maintenance or expansion at the WWTP whereupon effluents are directly released into the river system under conditions of low flow.

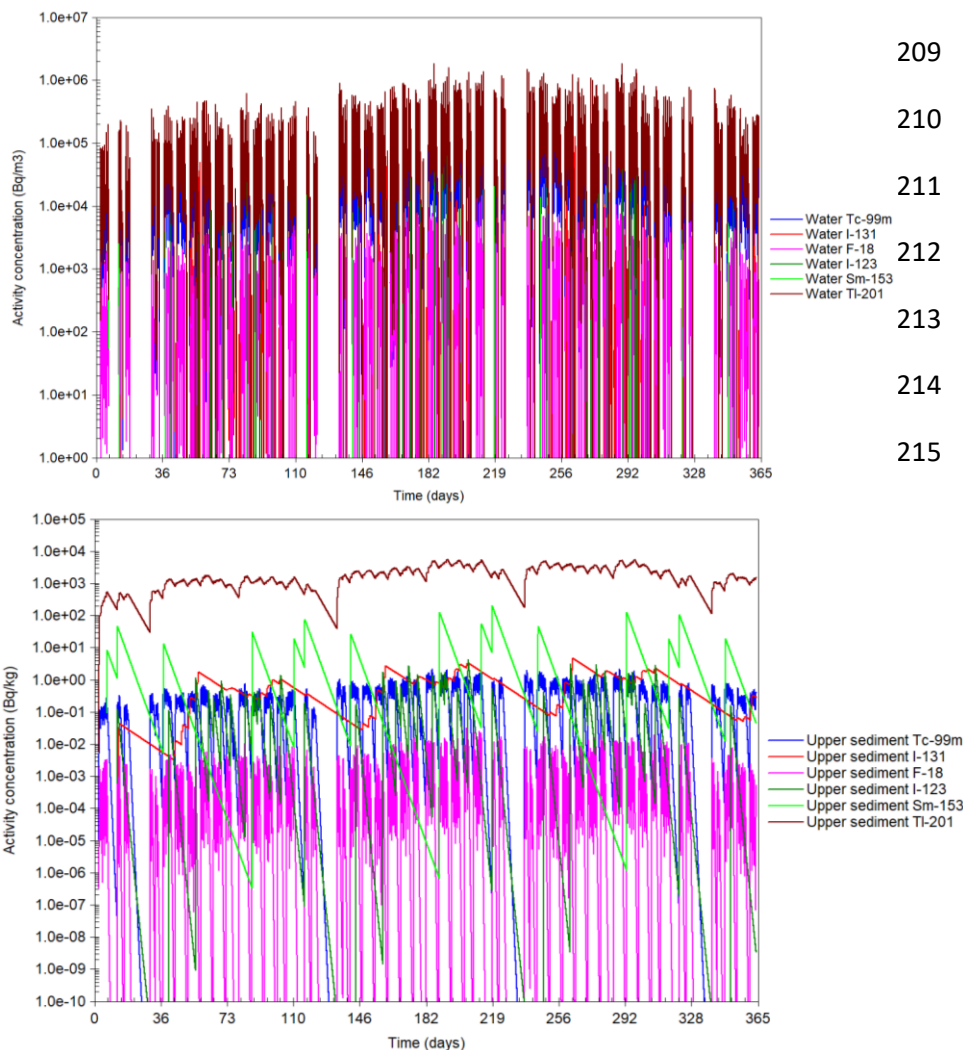


Figure 2: Activity concentrations in Molsse Nete river water in 2018 used as source term for the modelling (above) and modelled concentrations in sediment (below)

225

226 The activity concentrations in water exhibit daily fluctuations directly related to the activities of the  
227 hospital discharges. The principal radionuclides in terms of activity concentration in water (by two  
228 orders of magnitude) are  $^{201}\text{Tl}$ , followed by  $^{123/131}\text{I}$  and  $^{99\text{m}}\text{Tc}$ ,  $^{18}\text{F}$  and the remainder. For sediment, the  
229 order is  $^{201}\text{Tl}$ ,  $^{153}\text{Sm}$ , then  $^{131}\text{I}$  and  $^{99}\text{Tc}$ ,  $^{18}\text{F}$  and the remaining radionuclides. The time-integrating action  
230 of the sediment smoothens somewhat the oscillating water radionuclide levels, especially for  $^{201}\text{Tl}$  and  
231  $^{153}\text{Sm}$ . Note that for the calculation of activity in upper sediment, we used an indicative reworking rate  
232 of  $1.37 \times 10^{-5} \text{ m d}^{-1}$ , typical of shallow environments (Simmonds et al., 2004).

233 Figure 3 gives the dynamically modelled activity concentration of  $^{18}\text{F}$ ,  $^{99\text{m}}\text{Tc}$ ,  $^{123}\text{I}$ ,  $^{131}\text{I}$ ,  $^{153}\text{Sm}$ , and  $^{201}\text{Tl}$   
234 in pelagic & benthic fish, crustaceans, mollusc, macro-algae, phytoplankton and zooplankton. From this  
235 figure, it can be seen that  $^{18}\text{F}$ ,  $^{99}\text{Tc}$ ,  $^{153}\text{Sm}$  and  $^{201}\text{Tl}$  concentrate principally in plankton, whereas for  $^{123}\text{I}$   
236 and  $^{131}\text{I}$ , the radionuclide concentrates principally in fish. The activity concentrations display maxima in  
237 the order of magnitude  $10^6$  ( $^{201}\text{Tl}$ ),  $10^4$  ( $^{18}\text{F}$ ,  $^{99}\text{Tc}$  and  $^{153}\text{Sm}$ ) and  $10^3$  ( $^{123/131}\text{I}$ )  $\text{Bq kg}^{-1}$ .

238 The main transfer parameters used to derive the above activity concentrations are detailed in Tables 1  
239 and 2. We used data from the ERICA Tool, either primary data or applying the Tool's deductive method  
240 based on analogues. For some radionuclides (in our assessment, this concerns I and Tc) there is an  
241 additional source containing element dependent environmental input parameters for the Category A  
242 waste disposal project in Belgium (Sweeck, 2022), including some transfer parameters that cannot be  
243 found in IAEA TRS472 (IAEA, 2010). The reported  $K_d$  values for these radionuclides are  $10^{-1}$  and  $1.0$   
244  $\times 10^{-2} \text{ m}^3 \text{ kg}^{-1}$ , respectively (or  $3.6 \text{ m}^3 \text{ kg}^{-1}$  if Mo and Tc are considered as analogues, as recommended  
245 here). Whilst drawing attention to this source, we retain the results obtained with the ERICA method  
246 because (a) the values used are either similar or more conservative, (b) there is consistency with the  
247 calculation approach for the other radionuclides for which there are no data in the Belgian source, and  
248 (c) an assessment for an European scenario would tend to use the ERICA values. A similar situation  
249 occurs for the concentration factors. The Belgian best-estimate CF for fish are  $10^{-1} \text{ m}^3 \text{ kg}^{-1}$  for I and  $1.5$   
250  $\times 10^{-2}$  for Tc, compared with the values in our database of  $3.1 \times 10^{-1}$  and  $9.9 \times 10^{-2} \text{ m}^3 \text{ kg}^{-1}$ , respectively,  
251 which again implies a higher degree of conservatism for the parameters in our database, as desired.

### 252 3.1.2 Dose rates to the wildlife

253 The dynamically modelled dose rates of  $^{18}\text{F}$ ,  $^{99\text{m}}\text{Tc}$ ,  $^{123}\text{I}$ ,  $^{131}\text{I}$ ,  $^{153}\text{Sm}$ , and  $^{201}\text{Tl}$  to pelagic & benthic fish,  
254 crustaceans, mollusc, macro-algae, phytoplankton and zooplankton, unweighted by radiation quality,  
255 are given in Fig. 4. This figure gives the total dose rate, summing of internal and external exposures  
256 (according to our simulations, internal exposure dominates over external by 2 – 3 orders of magnitude).  
257 The peaks in Figure 4 shows absolute maximum values of the order of magnitude  $10^{-1}$  ( $^{99}\text{Tc}$ ,  $^{123/131}\text{I}$ ,  
258  $^{153}\text{Sm}$ ),  $10^0$  ( $^{18}\text{F}$ ) and  $10^1$  ( $^{201}\text{Tl}$ )  $\mu\text{Gy h}^{-1}$  when using the generic and highly conservative source term  
259 calculated in this study.

260 In a dynamic situation like the one considered, peak maximum dose rates are not a meaningful quantity  
261 to measure the risk, because such dose rates are applied over a short time and lower dose rates prevail  
262 for most of the time. Rather, it is the integration of the dose rate received over a set of time divided by  
263 the time, i.e. the average dose, that should be used to compare with benchmark values of dose. The D-  
264 DAT model performs such a calculation for a time of 1 year, as shown in Fig. 5. For a given time T, the  
265 output is the average dose rate between  $t = \text{zero}$  and  $t = T$ , divided by T. In particular, we take the last  
266 point in the graph ( $T = 365$  days) to give an average dose rate for the period.

267 The following conclusions are evident from Fig. 5. Firstly, external exposures (in the order macroalgae  
268 > mollusc > benthic fish > phytoplankton and zooplankton > pelagic fish) are several orders of  
269 magnitude below internal exposures, which are in the order mollusc > phytoplankton > crustacean and  
270 benthic fish > zooplankton and pelagic fish > macroalgae. Secondly, the highest annually averaged dose  
271 rate (internal dose rate for mollusc, arising mainly from  $^{201}\text{Tl}$ ), at  $3.7 \mu\text{Gy h}^{-1}$ , is below the  $10 \mu\text{Gy h}^{-1}$   
272 incremental screening dose rate for risk characterisation from the ERICA methodology (Brown et al.,  
273 2016; Brown et al., 2008), with a risk quotient of 0.37.

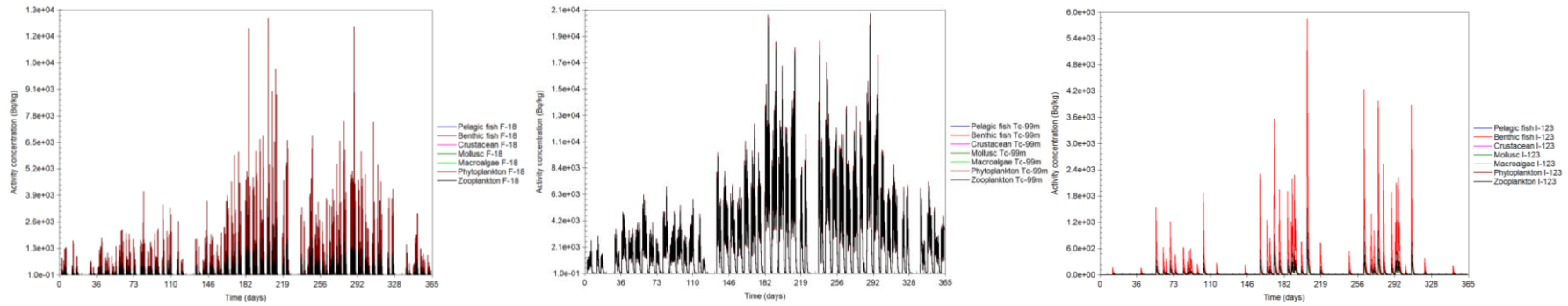
274 The object of protection within the ERICA Integrated Approach is that generic ecosystems are protected  
275 from structure and function effects under chronic exposures. The ERICA methodology proposes the  
276 aforesaid  $10 \mu\text{Gy h}^{-1}$  screening dose rate based on examination of data on effects of ionising radiation  
277 in wildlife (Coppstone et al., 2008; FREDERICA, 2006). This is not a limit: exceeding it means simply  
278 that the site under analysis cannot be screened-out from further detailed assessment. In our case,  
279 therefore, it is therefore possible to state that the aquatic biota are not at risk, especially considering that  
280 the dose rates are well below the lower level of the ICRP derived consideration reference level (DCRL)  
281 bands for biota (ICRP, 2008).

## 282 **3.2 Accidental $^{131}\text{I}$ release scenario**

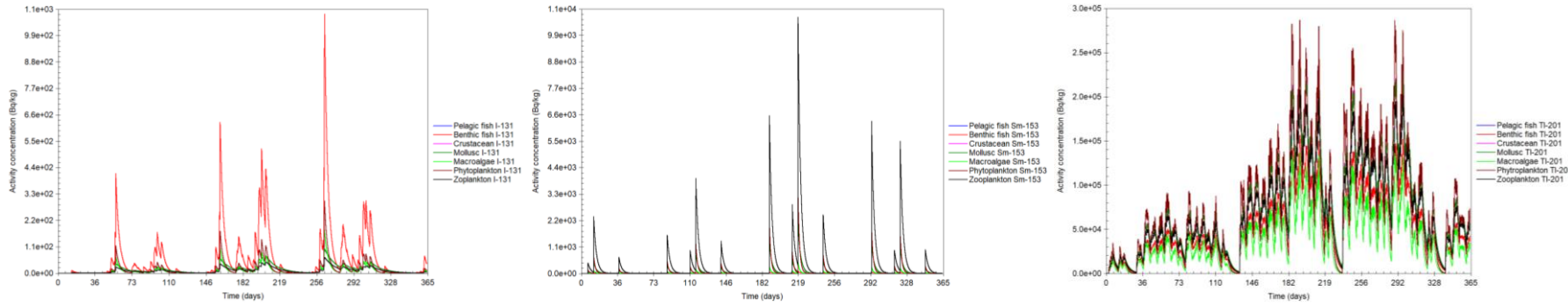
### 283 **3.2.1 Activity concentrations in water, sediment and the wildlife**

284 Fig. 6 gives the activity concentration in water and sediment per MBq  $^{131}\text{I}$  release directly into the sewer  
285 system (iodine pill release scenario), reaching the river at the outlet of the WWTP during plant shutdown  
286 when the river carries the lowest flow. This scenario can be scaled-up if desired, as the doses are  
287 proportional to release. The resulting time-dependent and time-averaged dose rates are given in Fig. 6.

288



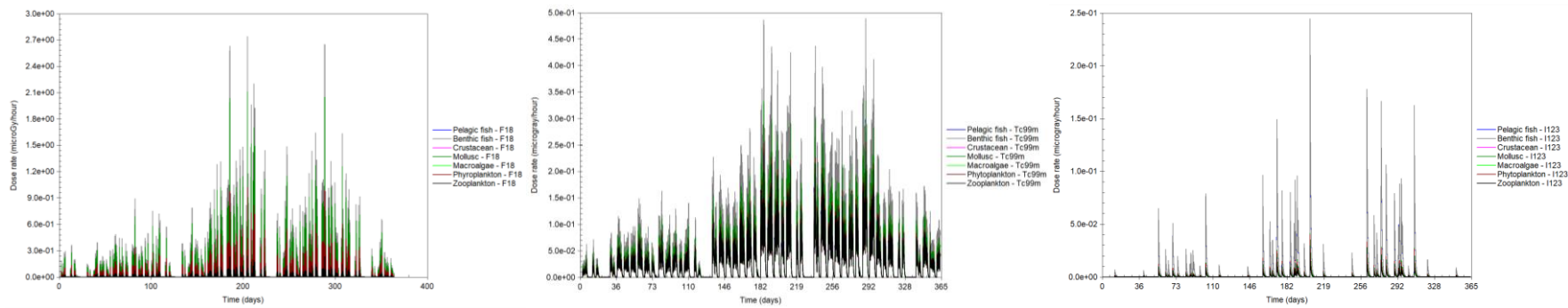
289



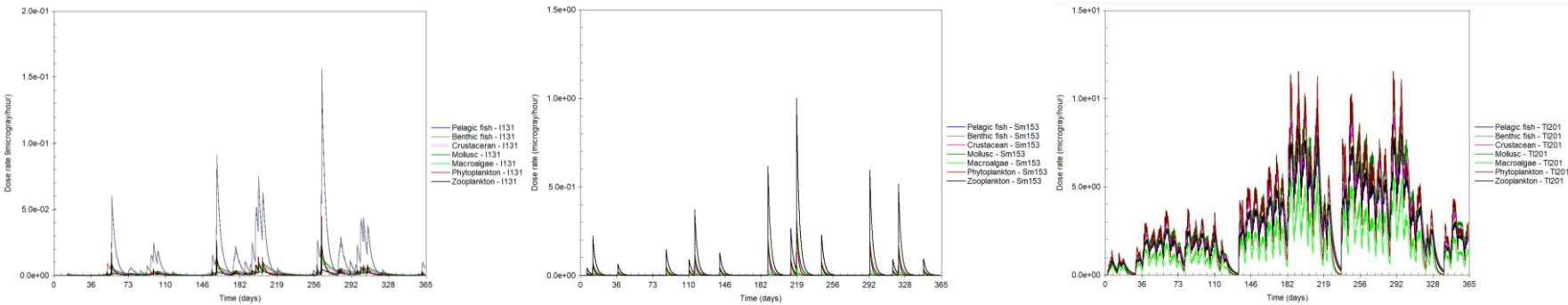
290 Figure 3: Dynamically modelled activity concentration of radionuclides in aquatic wildlife ( $\text{Bq kg}^{-1}$ ) from the Molsa Nete River

291

292



293



294

295 Figure 4: Dynamically modelled dose rates of radionuclides in aquatic wildlife ( $\mu\text{Gy h}^{-1}$ ) from the Molsa Nete River

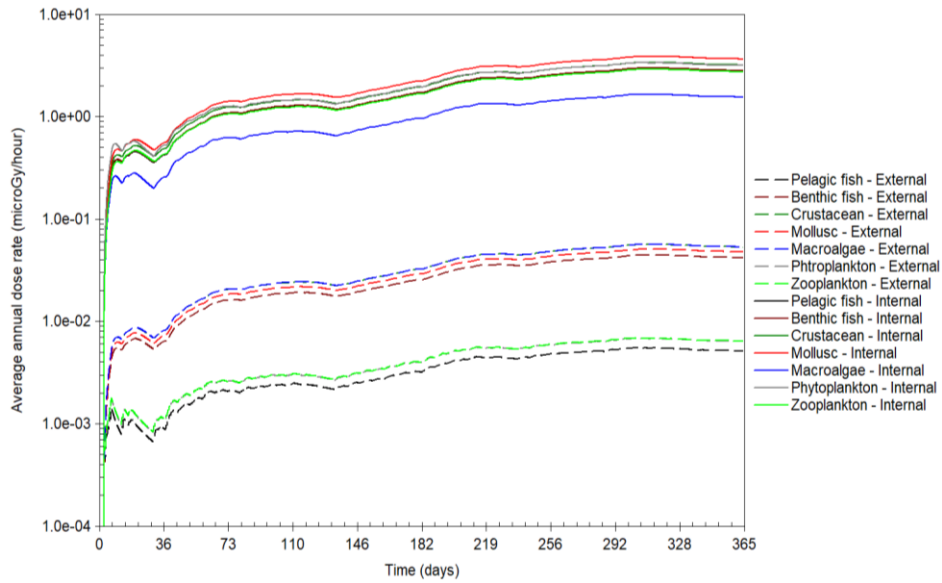


Figure 6: Time average of internal and external dose rates (sum of all radionuclides)

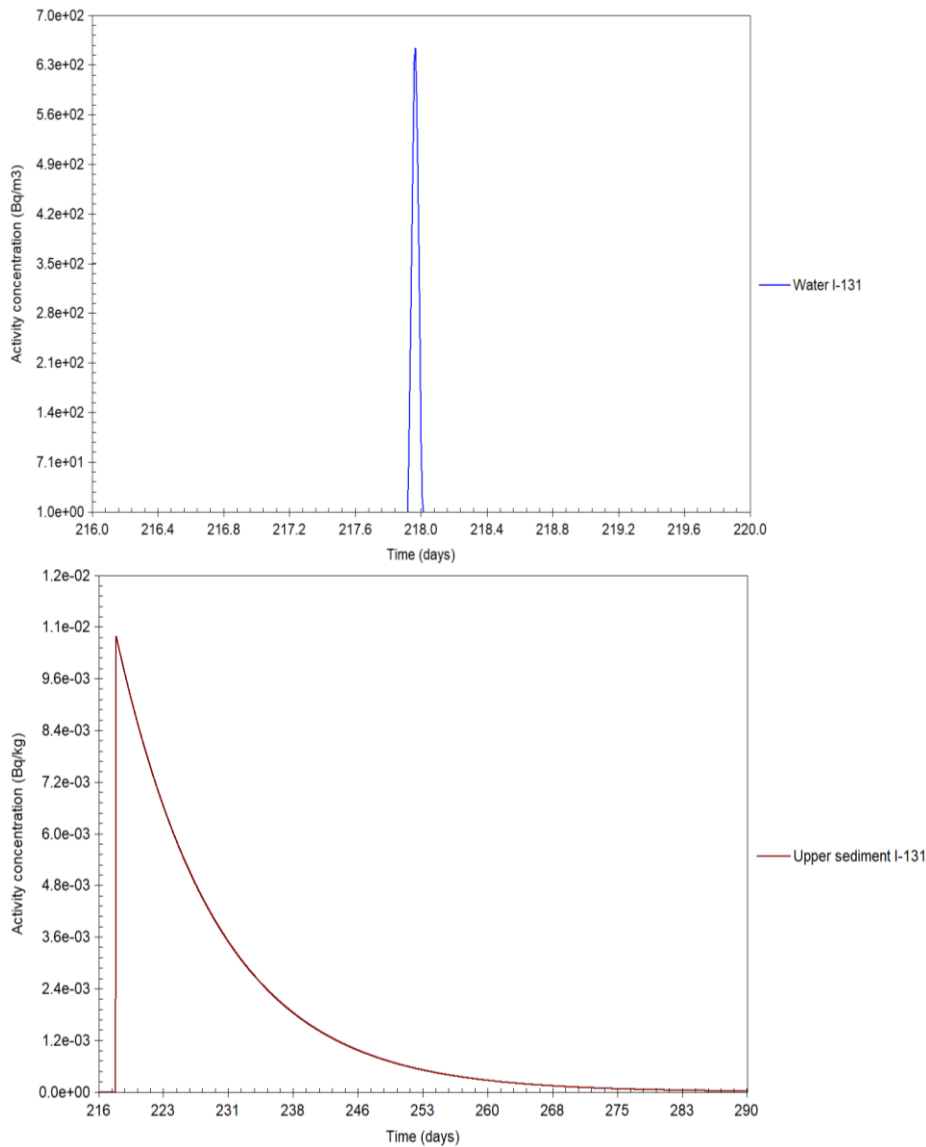


Figure 5: Modelled concentrations of <sup>131</sup>I in water (above) and sediment (below) for the accidental iodate pill release scenario

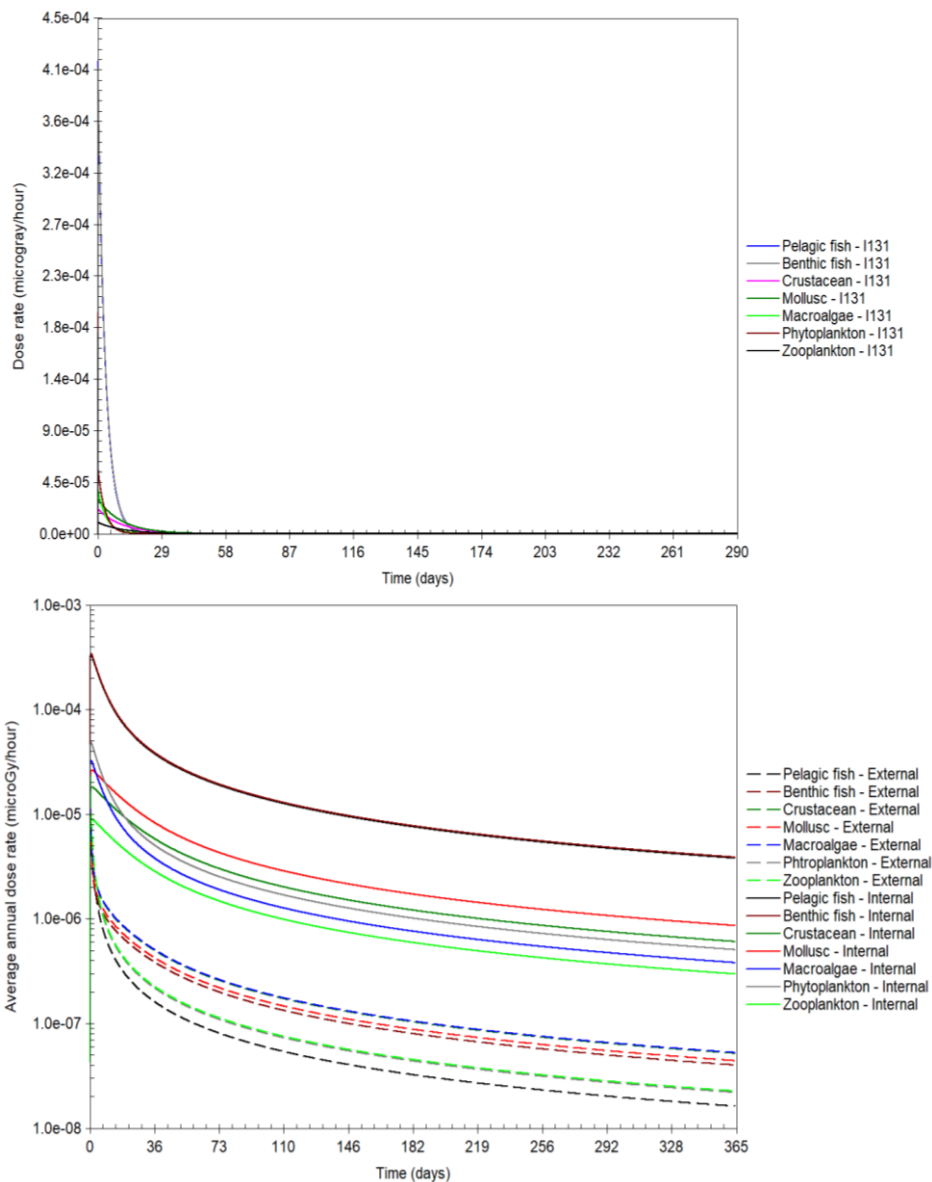


Figure 7: Modelled  $^{131}\text{I}$  in dose rate in biota (above) and integration of internal and external dose rates over a one year period following release, divided by the time period considered for the accidental iodate pill release scenario (below)

In Fig. 7, a coordinate change is made to place the peak at  $T = 0$  in order to be able to follow-up the decaying dose profile over a 1-year period after release. The 1-year averaging cut-off time is arbitrary of course, but dose rates for different integration periods can be extrapolated if desired from the given figures.

The conclusion that the exposures to non-human biota have no radiological significance whatsoever can be determined by consultation of these figures. The single peak of water concentration, with a maximum of  $654 \text{ Bq m}^{-3}$  at the Molse Nete river at  $T = 218$  days, and associated peak in sediment of a maximum of  $0.011 \text{ Bq kg}^{-1}$ , rapidly decay through the effects of delay and dilution. The maximal activity

concentration in biota is  $218 \text{ Bq kg}^{-1}$  for pelagic and benthic fish, with progressively lower concentrations of phytoplankton, macroalgae, crustacean and zooplankton (in that order).

### 3.2.2 Dose rates to the wildlife

The peak doses to the biota are of the order of  $4.1 \times 10^{-4} \mu\text{Gy h}^{-1}$  for pelagic and benthic fish followed by phytoplankton > macroalgae > crustacean and mollusc > zooplankton (Fig. 8). The one-year time-averaged dose rates are very low. For internal exposure, they are  $4 \times 10^{-6} \mu\text{Gy h}^{-1}$  for pelagic and benthic fish, decreasing to  $9 \times 10^{-7} \mu\text{Gy h}^{-1}$  for mollusc,  $6 \times 10^{-7} \mu\text{Gy h}^{-1}$  for crustacean,  $5 \times 10^{-7} \mu\text{Gy h}^{-1}$  for phytoplankton,  $4 \times 10^{-7} \mu\text{Gy h}^{-1}$  for macroalgae and  $3 \times 10^{-7} \mu\text{Gy h}^{-1}$  for zooplankton. External dose rates are one order of magnitude lower with the most exposed group being macroalgae, with a very low dose rate of  $5 \times 10^{-8} \mu\text{Gy h}^{-1}$ , and the least exposed group being pelagic fish at  $< 2 \times 10^{-8} \mu\text{Gy h}^{-1}$ . According to the methodology used here, such dose rates have no environmental significance. Hence, this type of accidental release scenario poses no significant risk to the environment.

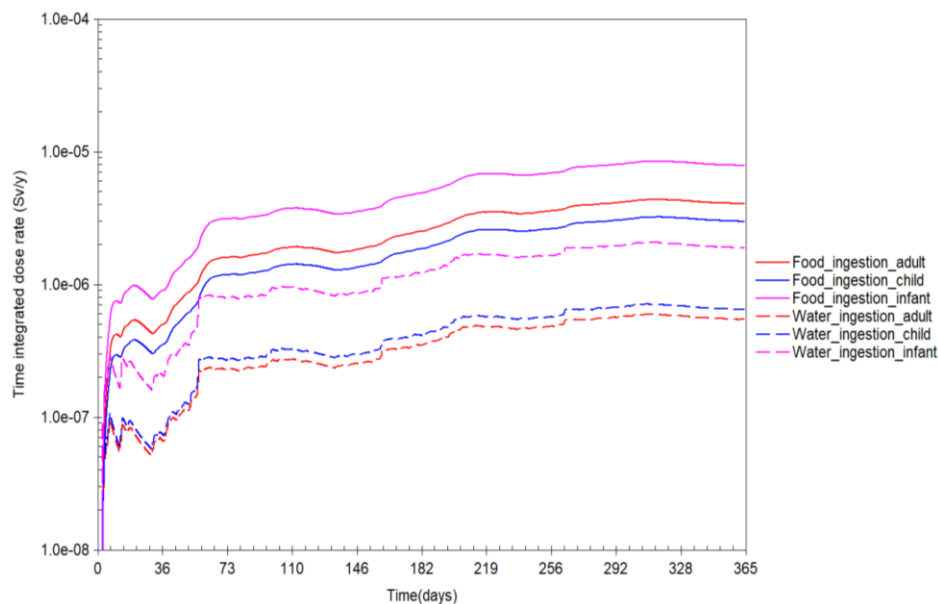


Figure 8: Time integrated ingestion dose rates for a routine discharge scenario, combining all radionuclides and food groups

## 3.3 Dose assessment for people

### 3.3.1 Doses to consumers and members of the public using the D-DAT dynamic model

The D-DAT model was used to calculate the dose rates to people of three age groups (adult, 10-year old and infant) arising from ingestion of water and of the biota, once consumption rates are set. The results are given in Fig. 9. D-DAT was also used to calculate the external dose rates from sediment (walking along the riverbank) and swimming exposure, as shown in Fig. 10.

The mean internal dose rates arising from ingestion of biota (mainly fish) at the Molse Nete river under the generic scenario considered over a 1-year period range between  $2 \times 10^{-3} \text{ mSv y}^{-1}$  for child to  $8 \times 10^{-3} \text{ mSv y}^{-1}$  for infant, the differences being caused by the different dose factors (reflecting the age-

dependent radiation sensitivity) and Belgian consumption rates for the different age groups. The mean internal dose rates from water ingestion are lower, ranging from  $5 \times 10^{-4} \text{ mSv y}^{-1}$  for adult to  $1 \times 10^{-3} \text{ mSv y}^{-1}$  for the infant.

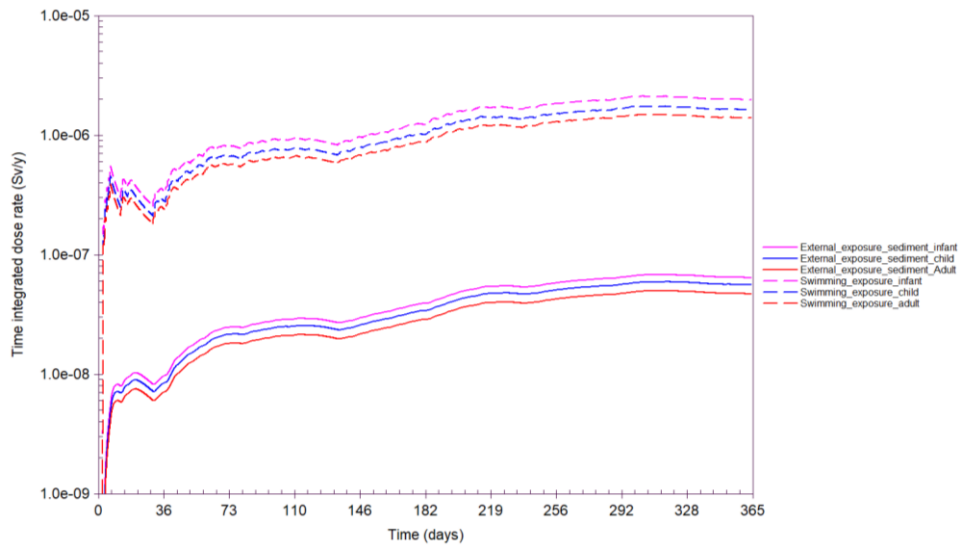


Figure 9: Time-integrated external exposure dose rates for a routine discharge scenario

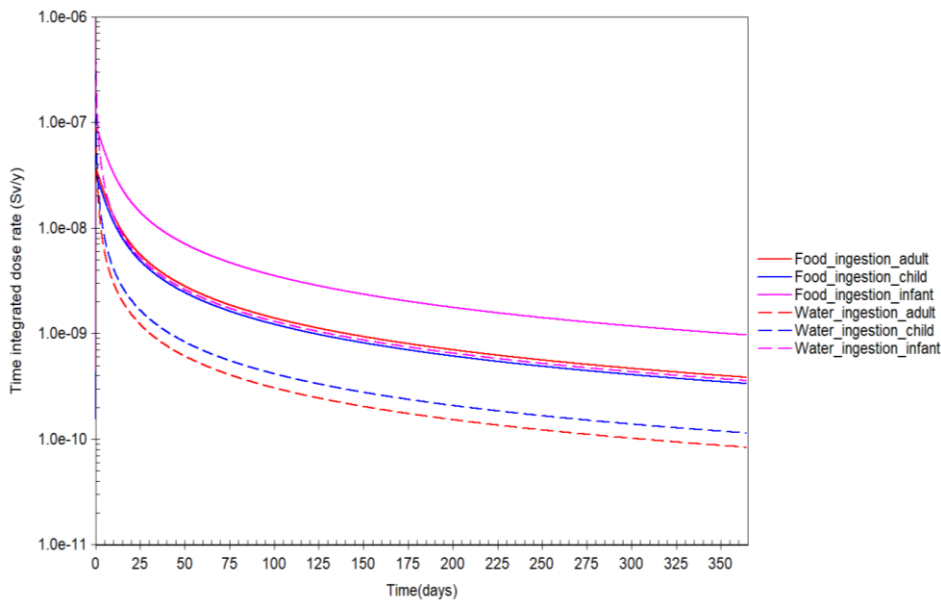


Figure 10: Time integrated ingestion dose rates for an accidental release of  $^{131}\text{I}$ , combining all radionuclides and food groups

The above dose rates are much lower than the worldwide average annual radiation dose rate from exposure due to naturally occurring radiation sources, including radon, of  $2.4 \text{ mSv}$  (UNSCEAR, 2000) and very close to  $10 \mu\text{Sv y}^{-1}$  which is considered a trivial dose in terms of risk (IAEA, 2014). These exposures are of no radiological significance whatsoever.

External exposures have the same implications. Exposure to sediment walking along the riverbank ranges between  $1.5 \times 10^{-3}$  mSv  $y^{-1}$  for adult and  $2 \times 10^{-3}$  mSv  $y^{-1}$  for the infant, due to age-related differences in dose factors. The dose rates for external exposure due to swimming are much lower, between  $5 \times 10^{-5}$  and  $6 \times 10^{-5}$  mSv  $y^{-1}$ . These dose rates are essentially trivial.

The  $^{131}\text{I}$  accident exposure scenario simulation gives significantly lower exposures compared with the routine scenario, as seen in Fig. 11. As we did in the assessment for biota, we placed the discharge at  $T = 0$  to perform integration over a complete year (the averaging cut-off time is arbitrary but doses for different integration periods can be obtained from the Figures). Modelled average dose rates after 1 year are several orders of magnitude below the trivial dose rate of  $10 \mu\text{Sv } y^{-1}$  indicating no radiological significance whatsoever for this situation.

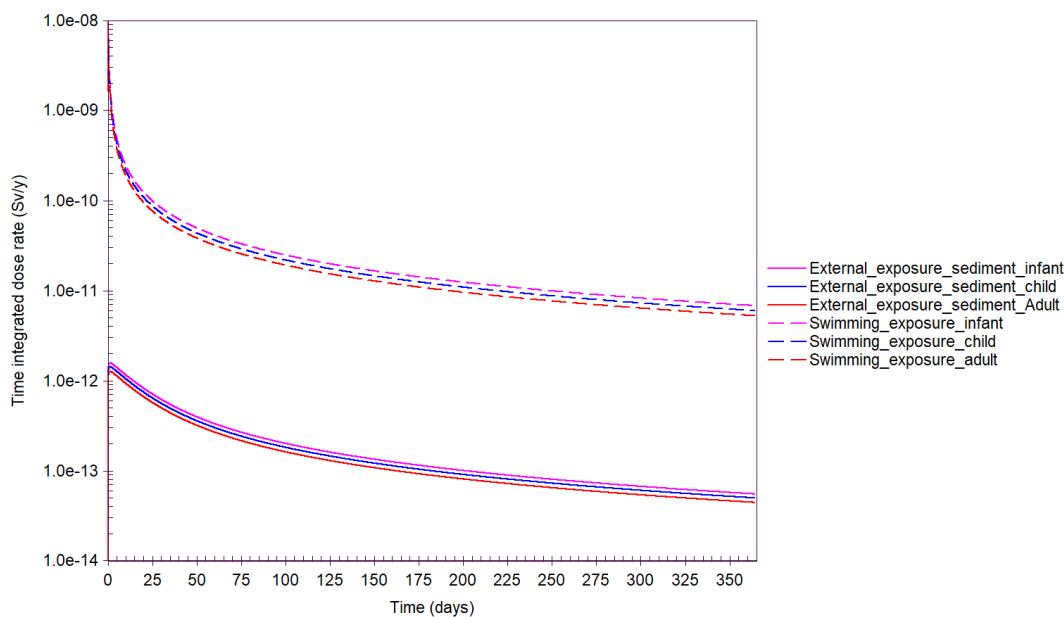


Figure 11: Time-integrated external exposure dose rates for an accidental release of  $^{131}\text{I}$

### 3.3.2 Doses to WTP workers and the public

#### 3.3.2.1 Fractionation of radionuclides

We made calculations of the doses to workers and the public at a Mol-sited water treatment plant which, unlike the Leuven plant, does not make the pessimistic assumption that radionuclides are diverted to the watercourse, but rather assume that the plant is operational, drawing water from the river. The main source of uncertainty in the dose assessment is the plant removal efficiency, that is, fraction of activity concentration entering the plant that is retained and thus separated from the effluent. Hence, the first step was to arrive at an estimate for these efficiencies.

The Belgian radiation protection regulator FANC performed automatic gamma spectrometric measuring stations at both inlet and outlet of several WWTPs in Belgium. This would, in theory, enable calculation of the efficiencies. However, in practice, it is not straightforward to do so because the detection limit

was approximately  $10^3 \text{ Bq m}^{-3}$ , sufficient in principle to detect the main radionuclides associated with hospital discharges ( $^{99\text{m}}\text{Tc}$ ,  $^{131}\text{I}$  and  $^{201}\text{Tl}$ ), but not others like  $^{18}\text{F}$ ,  $^{123}\text{I}$ ,  $^{153}\text{Sm}$  (Fiengo Pérez et al., 2022). The problem is compounded by not knowing the transit time of the different effluent fractions – for indicative purposes, a transition time of 15 hours is assumed for liquid effluent and 17 days are assumed for conditioned sewage sludge, which are treated for long enough to make them suitable for application to land (EA, 2022). All these factors can distort the calculation of the removal efficiencies, given the short half-life of the radionuclides involved.

We decided that it was preferable to source the (radionuclide-dependent) WWTP fractionation parameters, for which a reference was found in the literature (McDonnell, 2004). The first parameter required is the removal efficiency of the sewage processing, that is, the fraction not exiting the installation (in our study, we assume for simplicity that there is no loss due to decay during the few hours that the radioactivity is in the WTP except for  $^{18}\text{F}$ ,  $^{99\text{m}}\text{Tc}$  and  $^{123}\text{I}$ ). The second parameter is the fraction of the initial effluent that ends-up in the produced sludge (incorporating estimated decay in all cases, meaning that the fraction of  $^{18}\text{F}$ ,  $^{99\text{m}}\text{Tc}$  and  $^{123}\text{I}$  is virtually zero). The data are given in Table 3. For  $^{18}\text{F}$  and  $^{123}\text{I}$  for which the reference gives no data, a 90% efficiency of removal for sewage is assumed by expert judgement, similar to  $^{99\text{m}}\text{Tc}$  due to considerations of chemistry and fast decay. For  $^{153}\text{Sm}$ , the same efficiency as for  $^{201}\text{Tl}$  is assumed, based on similar considerations.

Table 3: Fractionation of radionuclides in sewage treatment plants

Radionuclide	Fraction in sewage	Fraction in sludge
$^{18}\text{F}$	0.9	0
$^{99\text{m}}\text{Tc}$	0.9	0
$^{123}\text{I}$	0.9	0
$^{131}\text{I}$	0.2	0.05
$^{153}\text{Sm}$	0.8	0.01
$^{201}\text{Tl}$	0.8	0.01

The assessment was performed using average concentrations because it is too complex now to do otherwise and the data are too limited to perform a dynamic modelling as was done for the non-human biota. Based on an assumption of 1% of the activity captured in the blocked sewer scenario and the input data, we arrived at average activity concentrations in the different plant fractions, as shown in Table 4.

Table 4: Average activity concentrations in the different plant fractions

Radionuclide	Average activity concentration ( $\text{Bq m}^{-3}$ )			
	Blocked Sewer	Liquid phase	Sludge	River discharge
$^{18}\text{F}$	4.2E+04	3.8E+04	0.0E+00	4.3E+01
$^{99\text{m}}\text{Tc}$	8.3E+06	2.3E+06	0.0E+00	2.6E+03
$^{123}\text{I}$	2.9E+05	3.6E+04	0.0E+00	4.1E+01
$^{131}\text{I}$	2.0E+06	1.7E+04	3.0E+04	1.5E+02
$^{153}\text{Sm}$	1.1E+05	3.7E+03	1.4E+03	8.4E+00
$^{201}\text{Tl}$	3.1E+08	6.9E+06	2.5E+06	1.6E+04

### 3.3.2.2 Radiological exposures for the routine scenario

The radiation dose rates to general plant workers and sewer maintenance workers (repairing a blockage), are given in Table 5. It can be seen that the order of exposure is external gamma > ingestion > inhalation, and that dose rates due to maintenance work are an order of magnitude lower than for general work, mainly due to the lower occupancy rate. It can be seen also that the order of contribution by radionuclide to total exposure is  $^{201}\text{Tl} > ^{99\text{m}}\text{Tc} > ^{18}\text{F} > ^{131}\text{I} > ^{123}\text{I} > ^{153}\text{Sm}$ . Given that  $^{201}\text{Tl}$  is not a strong gamma emitter, with main gamma emissions of 70.8 keV (46.5%), 68.9 keV (27.4%) and 80.3 keV (20.5%), much of the resulting dose is likely reduced by shielding provided by walls, tanks and containers, leading to very low dose rates for workers. Nevertheless, the highest dose rate (plant worker, sum of all radionuclides) is  $58 \mu\text{Sv y}^{-1}$ , a small fraction of the dose from naturally occurring radiation sources, including radon, of 2.4 mSv (UNSCEAR, 2000). All maintenance worker doses, and the majority of doses to WWTP workers except the external gamma exposure to  $^{99\text{m}}\text{Tc}$  and  $^{201}\text{Tl}$ , are below the trivial dose level of  $10 \mu\text{Sv y}^{-1}$ .

Table 5: Dose rates to workers at the WWTP including general work and sewer maintenance

Radionuclide	Dose rate (mSv y <sup>-1</sup> )			Totals
	Ingestion	Inhalation	Ext. Gamma	
WWTP workers				
<sup>18</sup> F	1.90E-08	2.50E-09	2.20E-03	2.20E-03
<sup>99m</sup> Tc	5.00E-07	3.00E-08	1.40E-02	1.40E-02
<sup>123</sup> I	7.60E-08	2.90E-09	2.80E-04	2.80E-04
<sup>131</sup> I	1.00E-05	3.80E-07	1.00E-03	1.00E-03
<sup>153</sup> Sm	3.80E-08	3.50E-09	1.80E-05	1.80E-05
<sup>201</sup> Tl	8.90E-06	4.60E-07	4.00E-02	4.00E-02
Total	2.00E-05	8.80E-07	5.80E-02	5.80E-02
Maintenance workers				
<sup>18</sup> F	8.30E-11	1.90E-12	9.90E-06	9.90E-06
<sup>99m</sup> Tc	7.30E-09	7.80E-11	2.10E-04	2.10E-04
<sup>123</sup> I	2.40E-09	1.70E-11	9.10E-06	9.10E-06
<sup>131</sup> I	1.70E-06	1.10E-08	1.70E-04	1.70E-04
<sup>153</sup> Sm	3.10E-09	5.20E-11	1.50E-06	1.50E-06
<sup>201</sup> Tl	1.20E-06	1.10E-08	5.20E-03	5.20E-03
Total	2.90E-06	2.20E-08	5.60E-03	5.60E-03

Dose rates for the freshwater pathways are given in Table 6. The dose rates from drinking water, either WTP treated water or unfiltered river water at the release point, are of no radiological significance whatsoever. The fish ingestion and external gamma radiation doses in Table 7 provide a point of comparison with the doses for the same pathways as dynamically calculated by D-DAT. The main difference between the two is that the human dose calculator used here considers removal of a significant part of the radioactivity at the treatment plant entering at monthly averages, whereas D-DAT uses a dynamic calculation. The D-DAT dose rates are more conservative and should be used as primary results given that the model calculates radionuclide transfer dynamically.

Table 6: Dose rates for the freshwater pathways

Radionuclide	Dose rate (mSv y <sup>-1</sup> )			
	External gamma at the riverbank	Fish ingestion	Drinking WWTP treated water	Drinking unfiltered river water
<sup>18</sup> F	2.60E-06	1.40E-08	9.20E-07	1.50E-09
<sup>99m</sup> Tc	4.40E-04	3.60E-08	2.50E-05	4.10E-08
<sup>123</sup> I	3.80E-04	1.60E-08	3.60E-06	6.20E-09
<sup>131</sup> I	3.90E-03	6.40E-06	1.40E-03	2.40E-06
<sup>153</sup> Sm	8.90E-03	2.00E-10	2.20E-07	4.60E-09
<sup>201</sup> Tl	1.20E-01	3.60E-05	6.10E-04	1.10E-06
Total	1.30E-01	4.20E-05	2.00E-03	3.60E-06

The predicted concentrations for application of water in irrigation and resulting dose rates are shown in Table 7. Dose rates arising from use of WTP sludge as a ground fertiliser are shown in Table 8. Dose rates from use of sludge as fertiliser predominate over dose rates from irrigation, but in both cases, the total dose rates ( $7.1 \times 10^{-5}$  and  $2.9 \times 10^{-6}$  mSv y<sup>-1</sup>, respectively) are insignificant, being near the 10 µSv y<sup>-1</sup> trivial dose level.

Table 7: Predicted concentrations and resulting dose rates for the irrigation pathway

Radionuclide	Concentrations (Bq kg <sup>-1</sup> )		Dose rates (mSv y <sup>-1</sup> )		
	Green Vegetables	Root Vegetables	Green Vegetables	Root Vegetables	Total
<sup>18</sup> F	1.3E-04	6.2E-05	3.00E-10	3.50E-10	6.50E-10
<sup>99m</sup> Tc	2.2E-01	5.7E-02	2.20E-07	1.50E-07	3.70E-07
<sup>123</sup> I	1.3E-05	1.3E-05	1.20E-10	3.20E-10	4.50E-10
<sup>131</sup> I	7.1E-04	7.1E-04	7.00E-07	1.80E-06	2.50E-06
<sup>153</sup> Sm	1.9E-07	1.9E-07	6.40E-12	1.70E-11	2.30E-11
<sup>201</sup> Tl	7.4E-03	1.4E-03	3.20E-08	1.50E-08	4.70E-08
Total	2.3E-01	5.9E-02	9.60E-07	2.00E-06	2.90E-06

Table 8: Activity concentration in sludge and dose rates arising from use of WWTP sludge as a ground fertiliser

Radionuclide	Concentration (Bq kg <sup>-1</sup> )	Dose rate (mSv y <sup>-1</sup> )
<sup>18</sup> F	0.0E+00	0.0E+00
<sup>99m</sup> Tc	0.0E+00	0.0E+00
<sup>123</sup> I	0.0E+00	0.0E+00
<sup>131</sup> I	3.0E+01	1.0E-05
<sup>153</sup> Sm	1.4E+00	1.8E-08
<sup>201</sup> Tl	2.5E+03	6.1E-05
Total	2.5E+03	7.1E-05

### 3.3.2.3 Radiological exposures for the accidental scenario

For the accidental scenario, this method of calculating dose, based on a time average, is not naturally suited for a assessing a single isolated pulsed discharge. The integration period is by its nature arbitrary. In order to derive the average dose rate over the integration period, there is a need to use the average

activity concentration in water for that period. The time integrated dose rate is calculated and divided by the number of days of the integration period. For consistency with what was done in the routine scenario, we select this period to be one year.

The calculated  $^{131}\text{I}$  dose rates to regular and maintenance workers at the WWTP for a 1 year integration period are  $4.8 \times 10^{-7}$  and  $7.9 \times 10^{-8}$  mSv  $\text{y}^{-1}$ , respectively. For exposure to the public through the freshwater pathways, the dose rates from external gamma (riverbank occupancy), fish ingestion, drinking WWTP-processed water and drinking unfiltered river water are  $1.8 \times 10^{-6}$ ,  $2.9 \times 10^{-9}$ ,  $6.3 \times 10^{-7}$  and  $1.1 \times 10^{-9}$  mSv  $\text{y}^{-1}$ , respectively. Dose rates from ingesting green and root vegetables upon irrigation of farmland are  $3.2 \times 10^{-10}$  and  $8.3 \times 10^{-10}$  mSv  $\text{y}^{-1}$ , respectively. Finally, the dose rate arising from the use of WWTP sludge in agriculture is  $4.6 \times 10^{-9}$  mSv  $\text{y}^{-1}$ . All these dose rates are negligible, being significantly below the trivial dose level of  $10 \mu\text{Sv y}^{-1}$ .

#### 4. CONCLUSIONS AND RECOMMENDATIONS

In this project, we have made a practical demonstration of an approach for the environmental impact assessment of radiopharmaceuticals released from medical facilities, considering simultaneously both humans and the non-human biota, and able to dynamically calculate dose rates to non-human freshwater biota for short-lived hospital-sourced radionuclides, based on the biokinetic model D-DAT. We have also developed a method to calculate doses to water treatment plant workers and from agricultural practices in equilibrium conditions over a 1-year integration period.

We generated a radiological source term for a conservative scenario of radionuclides at the Belgian Molse Nete River during the low-flow year 2018, to symbolise typical environmental conditions likely to reach a WWTP from a hospital. The radionuclides covered ( $^{18}\text{F}$ ,  $^{123}\text{I}$ ,  $^{131}\text{I}$ ,  $^{153}\text{Sm}$ ,  $^{99\text{m}}\text{Tc}$  and  $^{201}\text{Tl}$ ) are the only ones for which environmental monitoring data were available. Additionally, a spike release of one MBq of  $^{131}\text{I}$  was used as a case for unplanned release, to simulate the accidental disposal of an iodate pill into the sewer system. Having trialled the approach with a generic source term, our method is now ready for use in realistic case studies.

All dose rates calculated in our maximising release scenario are low, even for the highly conservative scenario considered. In the case of biota, they do not exceed the ERICA predicted no effects dose rate of  $10 \mu\text{Gy h}^{-1}$ , meaning that no effects are expected at the population level for the fauna and flora in the Molse Nete River (and, by inference, in any other Belgian cases where the generalised concentrations of hospital-released radionuclides tend to be lower). For humans, the dose rates computed for the different exposure pathways are substantially below the  $2.4 \text{ mSv y}^{-1}$  public dose rate for all natural sources. In most cases, they are also below what is considered a trivial dose ( $10 \mu\text{Sv y}^{-1}$ ).

Nevertheless, it is not possible to state "case closed". It is necessary to continue to perform such assessments, since they are still infrequent due to the primary focus being on exposure to patients. In

addition, environmental exposures to medical radionuclides (and so discharges of radiopharmaceuticals in rivers) may increase with new nuclear therapies in the future. Moreover, occasional accidental discharges in European hospitals where higher concentrations are involved are not unheard of. There is a wider range of radionuclides to consider (e.g.  $^{89}\text{Zr}$ ,  $^{90}\text{Y}$ ,  $^{99}\text{Mo}$ ,  $^{131}\text{m}$ ,  $^{133}\text{Xe}$ ,  $^{177}$ ,  $^{177\text{m}}\text{Lu}$ ,  $^{223}$ ,  $^{226}\text{Ra}$ ,  $^{225}\text{Ac}$ , and  $^{227}\text{Th}$ ), and there is a need to bring down uncertainty in model parameters. Along the way, there is a need to improve and standardise modelling methods, in order to be able to explicitly demonstrate to regulators, the public and the relevant stakeholders that people and the environment are adequately protected.

In line with the above, we make the following specific recommendations so that the screening approach used here can be improved. Firstly, we believe that significant radiopharmaceutical industries and hospitals should conduct and publish annually their own environmental radioactivity monitoring, just as the nuclear industry does. There is a knowledge gap here, and significantly we had to resort to build our source term upon one of the few WWTPs where monitoring data is available to make our assessment, and environmental release data from actual hospitals could generally not be found.

Secondly, we recommend to extend the assessment approach to other radionuclides, which necessitates biokinetic research to establish the transfer parameters of the relevant radionuclides in their relevant physico-chemical chemical form (speciation) for biota (Vives i Batlle et al., 2022), which in the present study had to be deduced for some radionuclides, based on a chemical analogue methodology and other proven extrapolation methods. This research could involve aquatic tank experiments with freshwater biota, aiming at establishing transfer parameters (concentration factors and biological half-lives of elimination) for the radionuclides for which the data are not available and had to be deduced by applying extrapolation methods, especially for  $^{201}\text{Tl}$ .

Thirdly, there needs to be better knowledge of the *modus operandi* of water treatment plants to help better define the assessment scenario. We had to make certain (reasonably conservative) assumptions and simplifications to cover for a certain lack of generalisable plant process information. In order to reduce conservatism and minimise model conceptual uncertainties, there is need for actual knowledge of the retention/separation efficiencies of the different waste streams (water and sludge), as well as the basic working pattern (occupancy fractions) at the treatment plant in terms of worker hours per year spent between plant operation and plant maintenance. Other improvements needed include establishing the transit times of the different effluents to calculate accurately the relevant radionuclide decay factors, and also establishing what are the realistic shielding conditions for external beta and gamma exposure, which is especially important for  $^{201}\text{Tl}$  as this radionuclide appears to dominate external exposure to workers.

Finally, there should be a move towards a unified European approach for dose assessment from medical radionuclides, possibly by further developing the modelling methodology that we have developed in the

present project, so that different member states can be in a position to perform and compare assessments of the impact of radiopharmaceuticals on people and the environment using a consistent methodology. We particularly recommend that the environmental impact assessment approach should be part of the development process of radionuclide treatments.

## **ACKNOWLEDGEMENTS**

This project has received funding from the Euratom research and training programme 2019-2020 under grant agreement No 945196.

We thank Dr. Geert Biermans and Eng. Jurgen Claes from FANC for information and advice.

We also thank Dr. Sam Geerts from AQUAFIN, Eng. Joost Deweld from the VMM, Dr. Joris Vanlede Flanders Hydraulics for their advice and information provided.

We also wish to acknowledge Dr. Hugo Lepage, Dr. Patrick Boyer and Dr. Rodolfo Gurriaran from IRSN for allowing us to use the Rhône's River datasets for our model verification.

## REFERENCES

- Adamatzky, A. (2001) ModelMaker. *Kybernetes* 30, 120-125.
- Beresford, N.A., Beaugelin-Seiller, K., Burgos, J., M., C., Fesenko, S., Kryshev, A., Pachal, N., Real, A., Su, B.S., Tagami, K., Vives i Batlle, J., Vives-Lynch, S., Wells, C., Wood, M.D. (2015a) Radionuclide biological half-life values for terrestrial and aquatic wildlife. *Journal of Environmental Radioactivity* 150, 270-276.
- Beresford, N.A., Beaugelin-Seiller, K., Wells, C.V.-L., S., Vives i Batlle, J., Wood, M.D., Tagami, K., Real, A., Burgos, J., Fesenko, S., Cujic, M., Kryshev, A., Pachal, N., Su, B.S., Barnett, C.L., Uchida, S., Hinton, T., Mihalik, J., Stark, K., Willrodt, C., Chaplow, J.S. (2015b) A database of radionuclide biological half-life values for wildlife. NERC-Environmental Information Data Centre. <http://dx.doi.org/10.5285/b95c2ea7-47d2-4816-b942-68779c59bc4d>.
- Blaylock, B.G., Frank, M.L., (1981) Bioaccumulation and distribution of  $^{95m}\text{Tc}$  in an experimental freshwater pond. Report IAEA-SM-257/41. International Atomic Energy Agency, Vienna.
- Brown, J., Alfonso, B., Avila, R., Beresford, N., Copplestone, D., Hosseini, A. (2016) A new version of the ERICA tool to facilitate impact assessments of radioactivity on wild plants and animals. *Journal of Environmental Radioactivity* 153, 141-149.
- Brown, J.E., Alfonso, B., Avila, R., Beresford, N.A., Copplestone, D., Pröhl, G., Ulanovsky, A. (2008) The ERICA Tool. *Journal of Environmental Radioactivity* 99, 1371-1383.
- Brown, J.E., Beresford, N.A., Hosseini, A. (2013) Approaches to providing missing transfer parameter values in the ERICA Tool: how well do they work? *Journal of Environmental Radioactivity* 126, 399-411.
- Chapra, S.C. (1997) *Surface Water-Quality Modeling*. Waveland Press, Long Grove, IL.
- Citra, M.J. (1997) Modelmaker 3.0 for Windows. *Journal of Chemical Information and Computer Sciences* 37, 1198-1200.
- Copplestone, D., Hingston, J.L., Real, A. (2008) The development and purpose of the FREDERICA radiation effects database. *Journal of Environmental Radioactivity* 99, 1456-1463.
- EA, (2022) Initial radiological assessment tool 2: part 2 methods and input data. Chief Scientist's Group report, Environment Agency, Bristol, 403 pp.
- Eckerman, K.F., Ryman, J.C., (1993) External Exposure To Radionuclides In Air, Water, And Soil. Federal Guidance Report No. 12, EPA-402-R-93-081, p. 238 pp.
- FANC, (2015) Report of the campaign on direct measurements (immersed gamma-ray spectrometer probes) conducted at water treatment plants draining waste water from nuclear medical sector. FANC/AFCN, p. 28.
- Fiengo Pérez, F., Sweeck, L., Vives i Batlle, J., (2022) Deliverable D3.4 - Radionuclide dispersion simulations results. Radiation risk appraisal for detrimental effects from medical exposure during management of patients with lymphoma or brain tumour (SINFONIA) Euratom Project 945196, 59 pp.
- FREDERICA, (2006) FREDERICA Radiation Effects Database. Available from: <http://www.frederica-online.org/mainpage.asp>.
- Hervouet, J., M. (2007) *Hydrodynamics of Free Surface Flows*. John Wiley & Sons, Ltd.
- Hevland, M.E., (1981) Radiotechnetium as an environmental contaminant: Metabolism by two freshwater species, the pearl mussel (*Margaritifera margaritifera*) and the roughskinned newt (*Taricha granulosa*). Master's thesis. Corvallis, Oregon State, University. 64 pp.
- IAEA, (2001) IAEA. Generic models for use in assessing the impact of discharges of radioactive substances to the environment. IAEA Safety Reports Series 19. International Atomic Energy Agency, Vienna. Available from <https://www.iaea.org/publications/6024/generic-models-for-use-in-assessing-the-impact-of-discharges-of-radioactive-substances-to-the-environment>

- IAEA, (2009) Technetium-99m Radiopharmaceuticals: Status and Trends. International Atomic Energy Agency Radioisotopes and Radiopharmaceuticals Series No. 1, Vienna, 360 pp.
- IAEA, (2010) Handbook of parameter values for the prediction of radionuclide transfer in terrestrial and freshwater environments. Technical Reports Series No. 472. International Atomic Energy Agency, Vienna. Available from [https://www-pub.iaea.org/mtcd/publications/pdf/trs472\\_web.pdf](https://www-pub.iaea.org/mtcd/publications/pdf/trs472_web.pdf) [Accessed 22 Oct. 2020], Vienna.
- IAEA, (2014) Radiation Protection and Safety of Radiation Sources: International Basic Safety Standards. IAEA Safety Standards Series No. GSR Part 3, International Atomic Energy Agency, Vienna, 436 pp.
- ICRP, (1996) ICRP Publication 72: Age-dependent Doses to the Members of the Public from Intake of Radionuclides: Part 5. Compilation of Ingestion and Inhalation Dose Coefficients. International Commission on Radiological Protection, Pergamon Press, Oxford.
- ICRP, (2008) Environmental Protection: The Concept and use for Reference Animals and Plants. International Commission on Radiological Protection Publication 108, Annals of the ICRP 38(4-6), Elsevier Ltd., 76 pp.
- ICRP, (2012) ICRP Publication 119: Compendium of Dose Coefficients based on ICRP Publication 60. C.H. Clement (Ed.), Annals of the ICRP 41(1), 129 pp.
- ICRP (2014) Protection of the Environment under Different Exposure Situations. ICRP Publication 124, Annals of the ICRP 43(1).
- ICRP (2017) Dose Coefficients for Non-human Biota Environmentally Exposed to Radiation. International Commission on Radiological Protection Publication 136. Annals of the ICRP 46, 1-136.
- Lepicard, S., Heling, R., Maderich, V. (2004) POSEIDON/RODOS models for radiological assessment of marine environment after accidental releases: application to coastal areas of the Baltic, Black and North Seas. *Journal of Environmental Radioactivity* 72, 153-161.
- Lepicard, S., Raffestin, D., Rancillac, F. (1998) POSEIDON: A dispersion computer code for assessing radiological impacts in a European sea water environment. *Radiation Protection Dosimetry* 75, 79-83.
- Mahmood, Z.U.W., Norfaizal, M., Abu Bakar, N.S., (2014) Laboratory Bioaccumulation, Depuration And Total Dose Rate Of Waterborne Th-232 In Freshwater Fish Of *Anabas Testudineus*. In: Research and Development Seminar 2014; Bangi (Malaysia), 14-16 Oct 2014. Oral presentation.
- Martínez, J., Peñalver, A., Baciú, T., Artigues, M., Danús, M., Aguilar, C., Borrull, F. (2018) Presence of artificial radionuclides in samples from potable water and wastewater treatment plants. *Journal of Environmental Radioactivity* 192, 187 - 193.
- McDonnell, C.E., (2004) Radiological assessments for small users. National Radiation Protection Board Report NRPB-W63, United Kingdom, 95 pp.
- McKenzie-Carter, M., (1985) Uptake and retention of technetium by two freshwater species, the crayfish *Pacifastacus leniusculus* and the snail *Juga silicula*. Thesis for the degree of Master of Science in General Science (Radiation Health), Oregon State University, 66 pp.
- Rigas, M.L. (2000) Software Review: Modelmaker 4.0. *Risk Analysis* 20, 543-544.
- Seaman, J.C., Kaplan, D.I., (2010) Chloride, Chromate, Silver, Thallium and Uranium Sorption to SRS Soils, Sediments, and Cementitious Materials. Report SRNL-STI-2010-00493, Savannah River National Laboratory, Aiken, SC, 18 pp.
- Simmonds, J.R., Bexon, A.P., Lepicard, S., Jones, A.L., Harvey, M.P., Sihra, K., S.P., N., (2004) Update of the MARINA Project on the radiological exposure of the European Community from radioactivity in North European marine waters. Annex D: Radiological Impact on EU Member States of Radioactivity in North European Waters. European Commission report, 190 pp.

Sweeck, L., (2018) Element-independent biosphere parameters. Project near surface disposal of category A waste at Dessel. Belgian Agency for Radioactive Waste and Enriched Fissile Materials (NIRAS-ONDRAF) report NIROND-TR 2008–28E V3, 76 pp.

Sweeck, L., (2022) Element dependent environmental input parameters for the biosphere model - Project near surface disposal of category A waste at Dessel. Belgian Agency for Radioactive Waste and Enriched Fissile Materials (ONDRAF/NIRAS) Report NIROND-TR 2008–26E Version 4, 308 pp.

Titley, J.G., Carey, A.D., Crockett, G.M., Ham, G.J., Harvey, M.P., Mobbs, S.F., Tournette, C., Penfold, J.S.S., Wilkins, B.T., (2000) Investigation of the sources and fate of radioactive discharges to public sewers. Environment Agency Technical Report EA-RD-TR-P-288, Environment Agency, Bristol, United Kingdom, 274 pp.

Tomczak, W., Boyer, P., Krimissa, M., Radakovitch, O. (2019)  $K_d$  distributions in freshwater systems as a function of material type, mass-volume ratio, dissolved organic carbon and pH. Applied Geochemistry 105, 68-77.

UNSCEAR (2000) Sources and effects of ionizing radiation, United Nations Scientific Committee on the Effects of Atomic Radiation, UNSCEAR 2000 Report to the General Assembly with Scientific Annexes, Volume I: Sources, Annex B Exposures from natural radiation source. United Nations, New York. [Available from [https://www.unscear.org/docs/publications/2000/UNSCEAR\\_2000\\_Annex-B.pdf](https://www.unscear.org/docs/publications/2000/UNSCEAR_2000_Annex-B.pdf)].

Veliscek Carolan, J., Hughes, C.E., Hoffmann, E.L. (2011) Dose assessment for marine biota and humans from discharge of  $^{131}\text{I}$  to the marine environment and uptake by algae in Sydney, Australia. Journal of Environmental Radioactivity 102, 953-963.

Vives Batlle, J., (2013) Further development of the transfer model D-DAT and of a batch dose calculation tool based on ERICA. Report for COMET Milestone MS-311, Contract Number: Fission-2012-3.4.1-604794, Brussels, 14 pp.

Vives Batlle, J., Wilson, R.C., Watts, S.J., Jones, S.R., McDonald, P., Vives-Lynch, S. (2008) Dynamic model for the assessment of radiological exposure to marine biota. Journal of Environmental Radioactivity 99, 1711-1730.

Vives i Batlle, J. (2016) Dynamic modelling of radionuclide uptake by marine biota: application to the Fukushima nuclear power plant accident. Journal of Environmental Radioactivity 151, 502-511.

Vives i Batlle, J., Aoyama, M., Bradshaw, C., Brown, J., Buesseler, K.O., Casacuberta, N., Christl, M., Duffa, C., Impens, N., Iosjpe, M., Masqué, P., Nishikawa, J. (2018) Marine radioecology after the Fukushima Dai-ichi nuclear accident: Are we better positioned to understand the impact of radionuclides in marine ecosystems? . Science of the Total Environment 618, 80-92.

Vives i Batlle, J., Beresford, N.A., Beaugelin-Seiller, K., Bezhenar, R., Brown, J., Cheng, J.J., Čujić, M., Dragović, S., Duffa, C., Fiévet, B., Hosseini, A., Jung, K.T., Kamboj, S., Keum, D.-K., Kryshev, A., LePoire, D., Maderich, V., Min, B.-I., Periañez, R., Sazykina, T., Suh, K.-S., Yu, C., Wang, C., Heling, R. (2016) Inter-comparison of dynamic models for radionuclide transfer to marine biota in a Fukushima accident scenario. Journal of Environmental Radioactivity 153, 31-50.

Vives i Batlle, J., Urso, L., Raskob, W., (2022) Identification and prioritisation of ALLIANCE and NERIS SRA topics relevant to medical radiation protection research. EURAMED Rocc-N-Roll deliverable D2.4, 10 pp.

Vives i Batlle, J., Wilson, R.C., Watts, S.J., Jones, S.R., McDonald, P., Vives-Lynch, S. (2008) Dynamic model for the assessment of radiological exposure to marine biota. Journal of Environmental Radioactivity 99, 1711-1730.

Zitko, V. (1975) Toxicity and pollution potential of thallium. Science of the Total Environment 4, 185-192.